SUPPORTING INFORMATION

Design, Synthesis and Characterization of Novel Tetra Substituted 2,3-Dihydrothiazole Derivatives as DNA and BSA Targeting Agents: Advantageous of Visible-light-induced Multicomponent Approach

Ranjana Aggarwal,[a,b]* Naman Jain,[a] Gyan Prakash Dubey,[a]

[a]Department of Chemistry, Kurukshetra University, Kurukshetra-136119, Haryana, India

[b]CSIR-National Institute of Science Communication and Policy Research,

New Delhi-110012, India

*Corresponding author:

Prof. Ranjana Aggarwal, CSIR-National Institute of Science Communication and Policy Research, New Delhi 110012, India, Tel: +91-9896740740

E-mails: *ranjana67in@yahoo.com*, *ranjanaaggarwal67@gmail.com*

TABLE of CONTENT

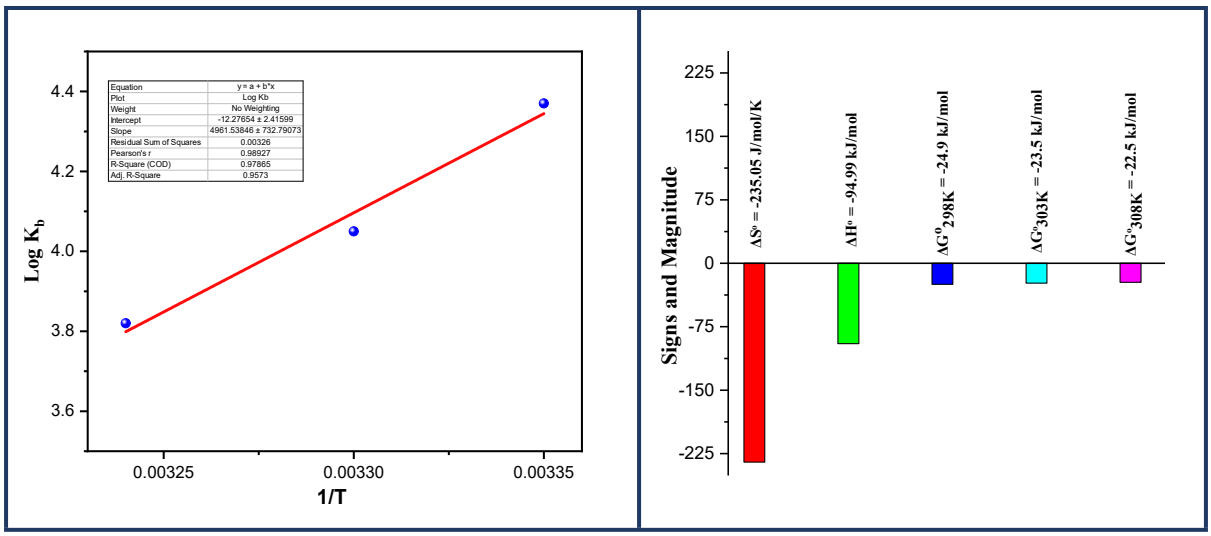

Figure SI. Van't Hoff plot for DNA-**6a** complex system and bar graph for the thermodynamic parameters ΔH^o, ΔS^o and ΔG^o.

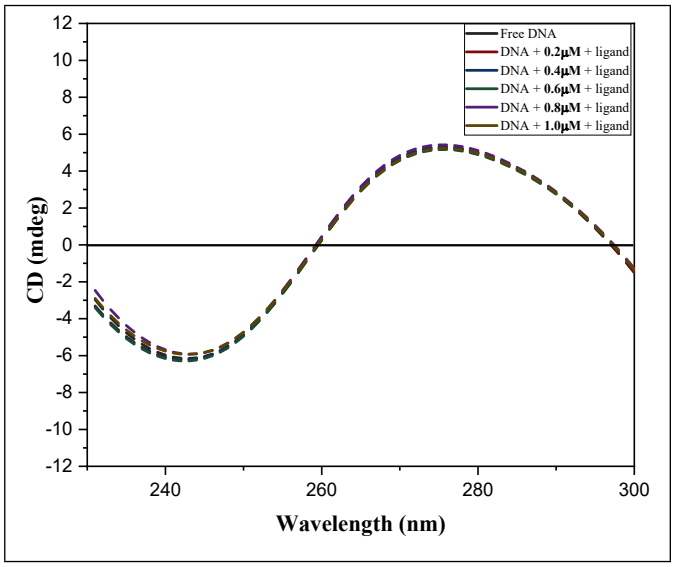

Figure S2. CD spectra of DNA in the absence and in the presence of an increasing concentration of ligand **6a** (0.2-1.0μM) at pH 7.2 and at 298 K.

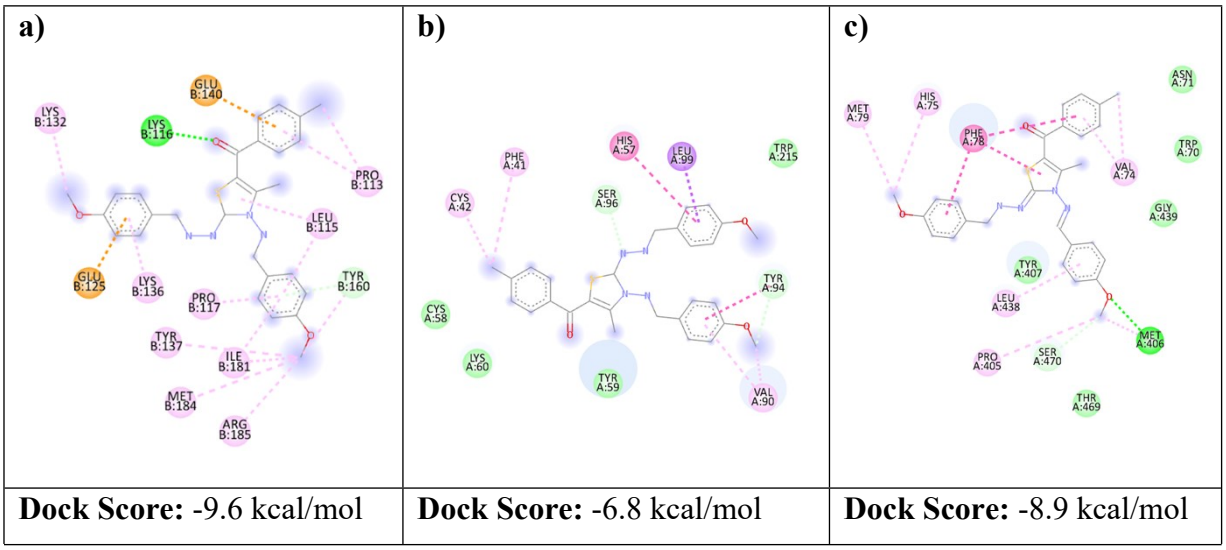

Figure S3 2D poses of the interaction of ligand **6a** with **a)** BSA, **b)** trypsin and **c)** glutathione.

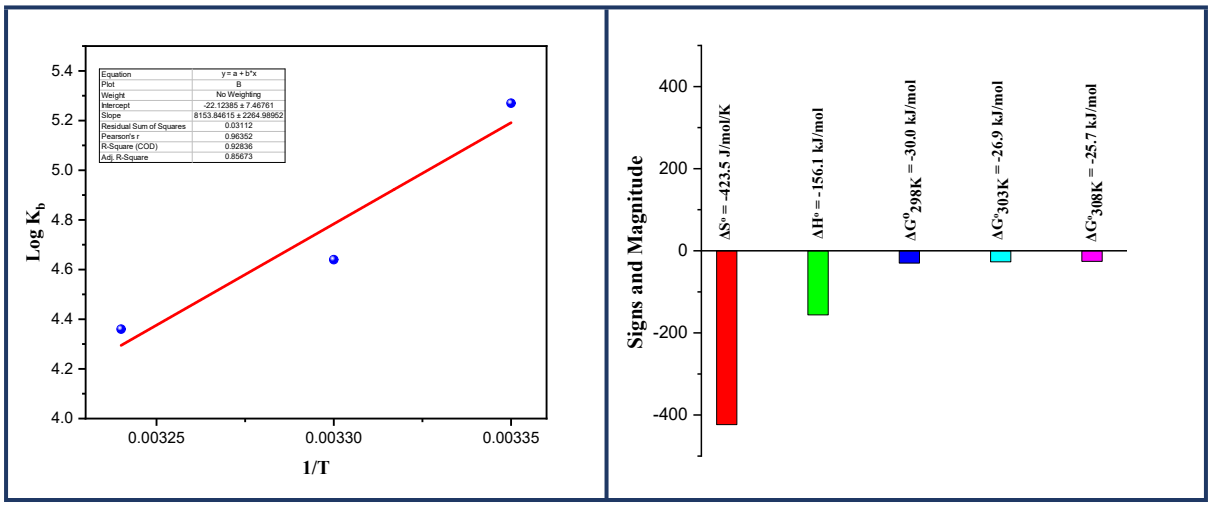

Figure S4. Van't Hoff plot for BSA-**6a** complex system and bar graph for the thermodynamic parameters ΔH^o, ΔS^o and ΔG^o.

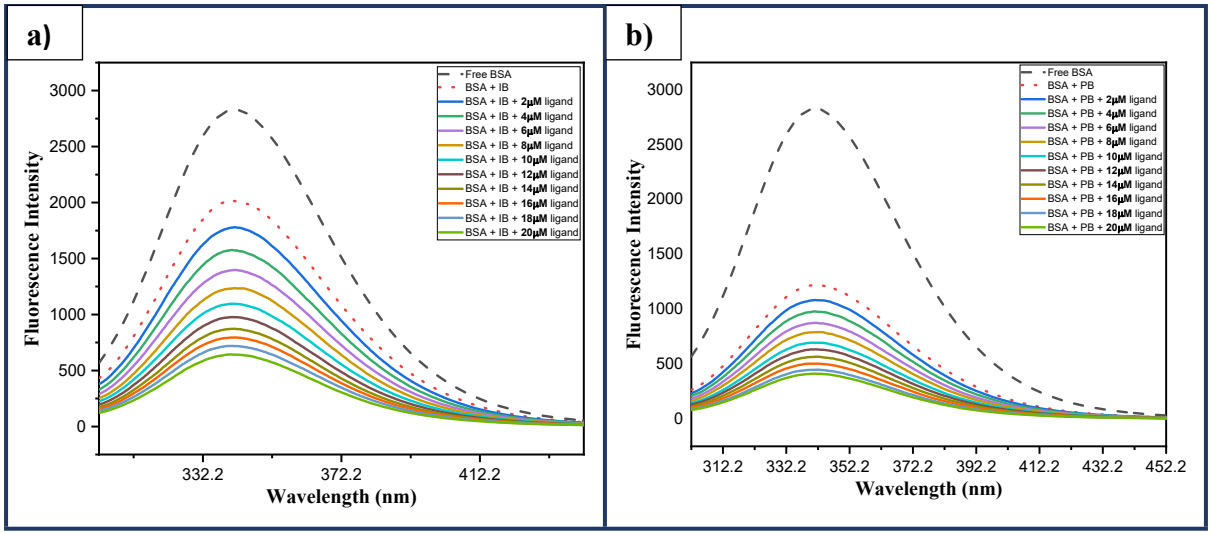

Figure S5. Fluorescence spectra of **a)** BSA-IB and **b)** BSA-PB complexes in the absence and presence of increasing concentration of **6a** (0-20μM) at 298 K.

Limit of Detection (LOD)

Detection limit has been calculated for each titration using the formula given below:

$$\text{Limit of Detection} = 3.3 \times \left(\frac{Standard\ Deviation\ of\ Slope}{Intercept} \right)$$

Table S1 highlights the value of LOD for both BSA and DNA at three temperature range 298K, 303K and 308K.

Table S1 LOD

Sr. No.	Temperature	Limit of Detection (ppm)	
		DNA	BSA
1.	298K	1.30	1.75
2.	303K	1.20	1.72
3.	308K	0.91	1.64

Experimental:

Chemistry

General Methods: Melting points were determined in open capillaries on digital Melting Point Apparatus (MEPA) and were uncorrected. Analytical TLC was performed using Merck Kieselgel 60 F254 silica gel plates. Visualization was performed by UV light (254 nm). The visible light source (White LED) used was of power 9W. IR spectra were recorded on Buck Scientific IR M-500 spectrophotometer using KBr pellets (υ_{max} in cm^{-1}), ^{1}H and ^{13}C NMR spectra were recorded on a Jeol ECZS-400 instrument at 400 and 100 MHz respectively using deuterated chloroform ($CDCl_3$) as a solvent and the chemical shifts are expressed in δ-scale and the coupling constant *J* is expressed in Hz downfield from TMS as internal standard. Also, 2D correlation spectra, (^{1}H-^{13}C) HMQC, (^{1}H-^{13}C) HMBC and (^{1}H-^{15}N) HMBC of samples **6a** and **6e** were carried out on a Jeol ECZS-400 instrument. Elemental analyses were performed at the Sophisticated Analytical Instrumentation Facility, Panjab University, Chandigarh. All the compounds gave C, H and N analysis within ±0.5 of the theoretical values. High-resolution mass spectra (HRMS) were measured in ESI^{+} mode at GJU, Hisar.

Binding Studies

Molecular docking studies

Primarily ligand structures were drawn using ChemDraw Professional 15.0 software and the crystal structure of the B-DNA dodecamer **(PDB ID: 1BNA)** and BSA protein **(PDB ID: 4F5S)** were attained from Protein Data Bank (https://www.rcsb.org/pdb). The protein file was then prepared for docking by removing water molecules and small residues like triethylene glycol and packing with polar hydrogen with Kollman charges using MGL Tools program. DNA receptor file was also prefixed in the same manner. In order to perform the molecular docking analysis Auto Dock Vina software 47 was used with grid size (BSA grid; center_x = 37.823, center_y = 23.992, center_z = 98.761; size_x = 126, size_y = 56, size_z = 74; energy_range = 4, exhaustiveness = 8) (DNA grid; center_x = 14.780, center_y = 20.976, center_z = 8.807; size_x = 92, size_y = 122, size_z = 126; energy_range = 4, exhaustiveness = 8) using the Lamarckian genetic algorithm for calculations, and the output results were analysed using the BIOVIA Discovery Studio Visualizer (DSV).

Material

Calf-thymus DNA (ct-DNA) of molecular biology ranking (fibers form), Bovine serum albumin and ethidium bromide (EtBr) were purchased directly from Sigma Aldrich Company and exploited without any absolution. Hoechst 33258 dye was procured from HiMedia. For the whole interaction studies, analytical grade reagents were used.

Stock solution preparation

For the preparation of a stock solution of **6a** having 2mM concentration, DMSO was used as a solvent and further diluted as per requirement depending upon the mode of interaction study. BSA stock solution of 13µM (1mg/1ml) concentration was prepared using Phosphate Buffer saline (prepared using Na_2HPO_4 and NaH_2PO_4) of 10mM concentration with pH 7.4. ct-DNA was homogenized by suspending in 10mM Tris-HCl buffer (pH 7.2, containing 0.1M HCl) with occasional mixing utilizing vortex. Beer-Lambert's Law ($A= \varepsilon lc$) was employed to determine the precise concentration of DNA at 260nm which was found to be 62µM using molar extinction coefficient (6600 $M^{-1}Cm^{-1}$) for an isolated strand of ct-DNA. The attenuance ratio A_{260}/A_{280} was found to be between 1.8 to1.9 using absorption spectroscopy indicative of protein-free DNA and thus there was no need for any kind of DNA purification.

Characterization of Final Compounds

^{1}H NMR, ^{13}C NMR, HMQC and HMBC Spectrum of Final Compounds

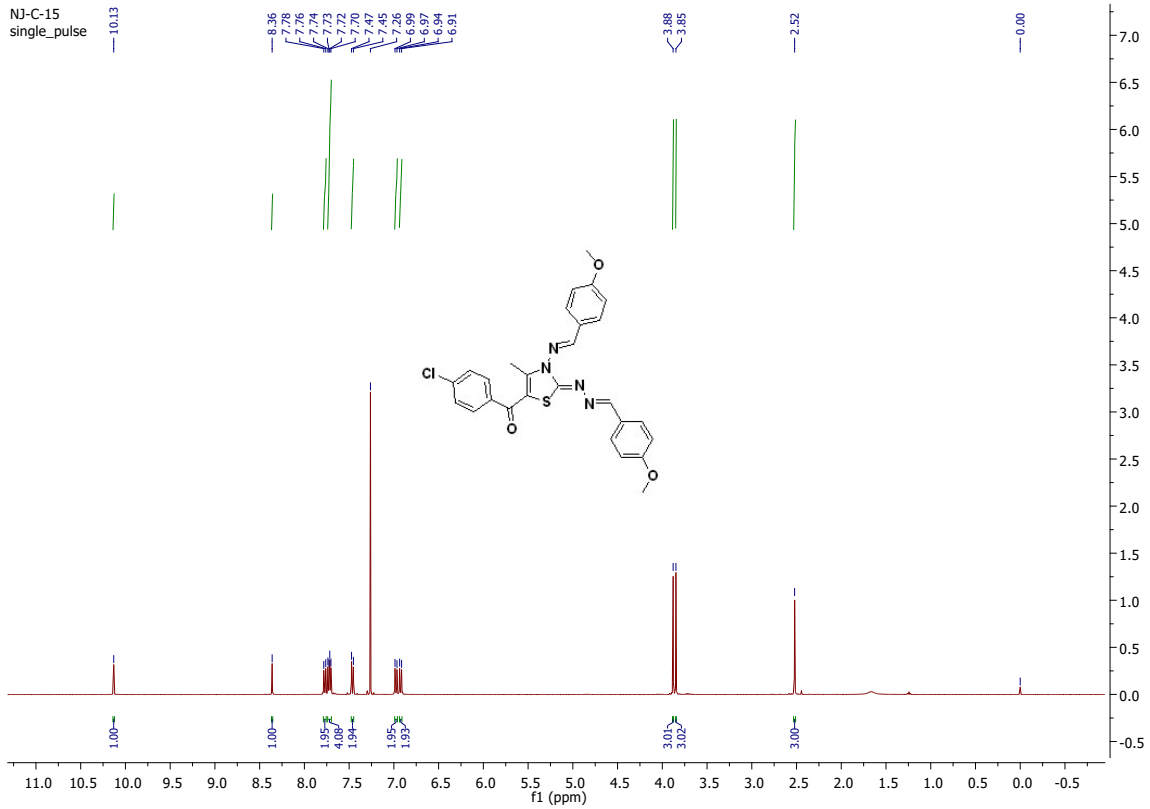

Figure S6. ^{1}H NMR spectrum of 6a

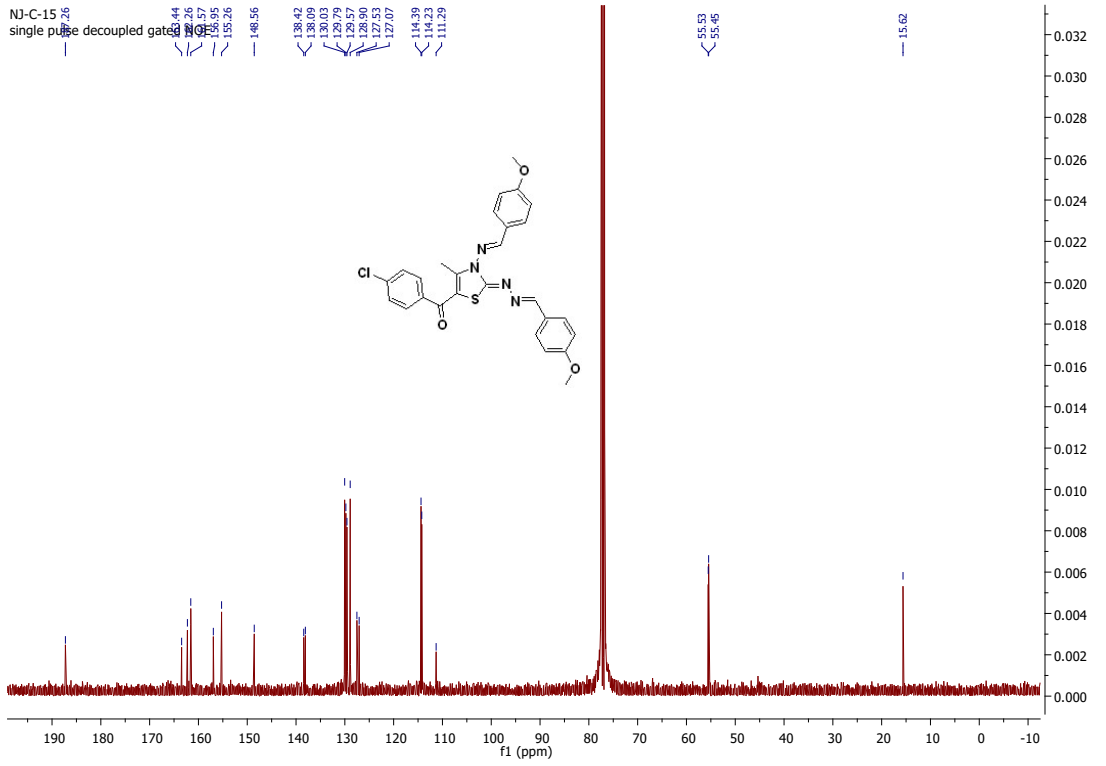

Figure S7. ^{13}C NMR spectrum of 6a

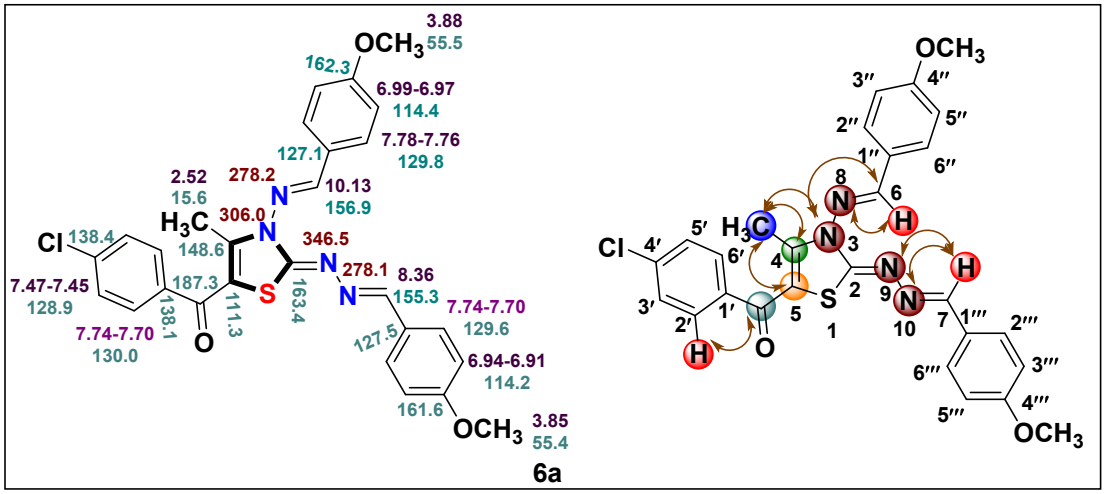

Table S2: 2D NMR correlation results for compound **6a**

Chemical shifts (δ in ppm)	gs-HSQC	gs-HMBC	Assignment
187.3	-	7.74-7.70 (H-2', 6')	CO
163.4	-	-	C-2
162.3	-	6.99-6.97 (H-3", 5") 3.88 (4"-OCH_3)	C-4"
161.6	-	6.94-6.91 (H-3"', 5"') 3.85 (4"'-OCH_3)	C-4"'
156.9	10.13 (H-6)	-	C-6
155.3	8.36 (H-7)	-	C-7
148.6	-	2.52 (4-CH_3)	C-4
138.4	-	7.47-7.45 (H-3', 5')	C-4'
138.1	-	7.74-7.70 (H-2', 6')	C-1'
130.0	7.74-7.70 (H-2', 6')	7.47-7.45 (H-3', 5')	C-2', 6'
129.8	7.78-7.76 (H-2", 6")	6.99-6.97 (H-3", 5")	C-2", 6"
129.6	7.74-7.70 (H-2"', 6"')	6.94-6.91 (H-3"', 5"')	C-2"', 6"'
128.9	7.47-7.45 (H-3', 5')	7.74-7.70 (H-2', 6')	C-3', 5'
127.5	-	7.74-7.70 (H-2"', 6"') 10.13 (H-6)	C-1"
127.1	-	7.78-7.76 (H-2", 6") 8.36 (H-7)	C-1"'
114.4	6.99-6.97 (H-3", 5")	7.78-7.76 (H-2", 6")	C-3"', 5"'
114.2	6.94-6.91 (H-3"', 5"')	7.74-7.70 (H-2"', 6"')	C-3", 5"
111.3	-	2.52 (4-CH_3)	C-5
55.5	3.88 (4"-OCH_3)	-	4"-OCH_3
55.4	3.85 (4"'-OCH_3)	-	4"'-OCH_3
15.6	2.52 (4-CH_3)	-	4-CH_3
346.5	-	8.36 (H-7)	9-N
306.0	-	10.13 (H-6) 2.52 (4-CH_3)	3-N
278.2	-	10.13 (H-6)	8-N
278.1	-	8.36 (H-7)	10-N

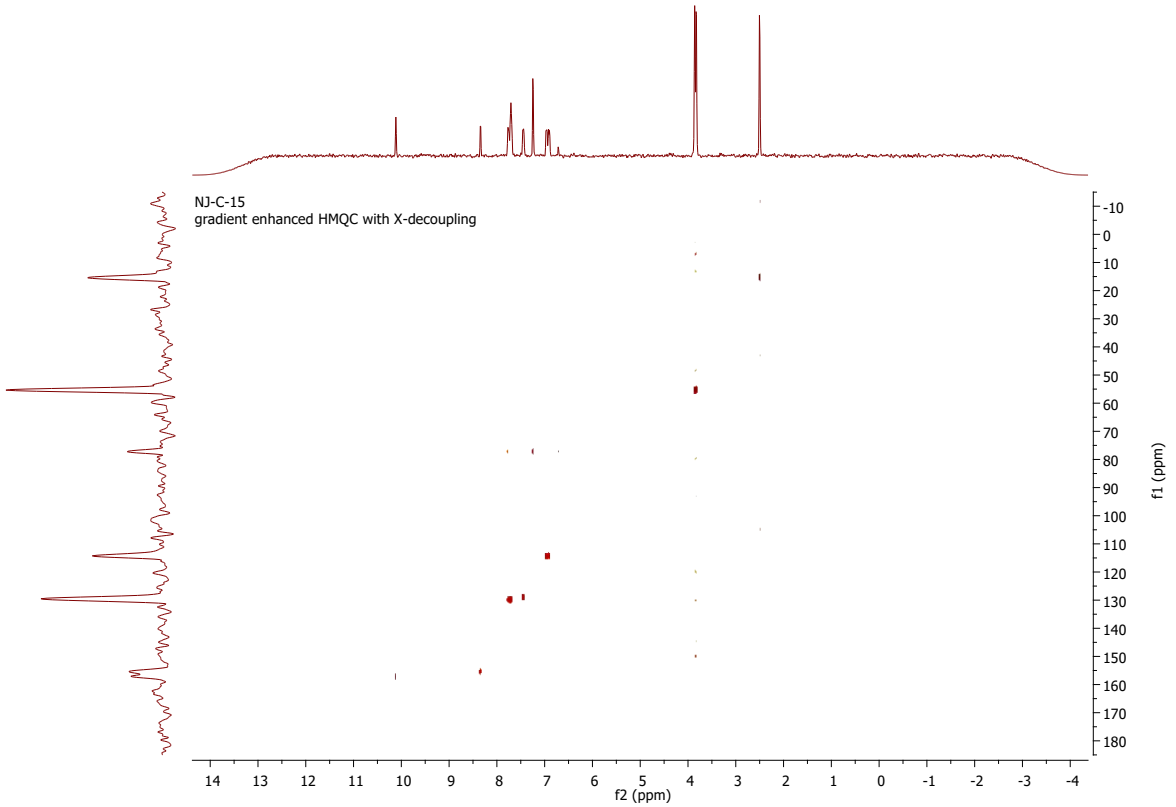

Figure S8. (^{1}H-^{13}C) HMQC NMR spectrum of 6a

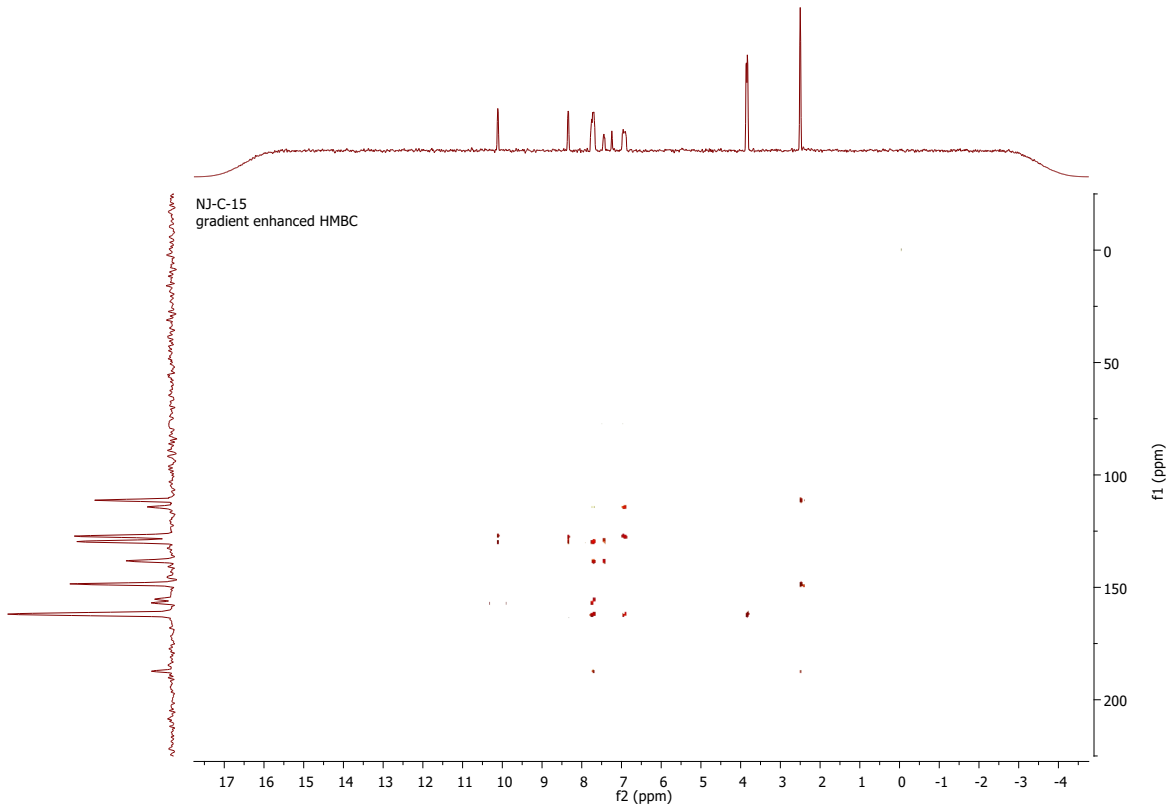

Figure S9. (^{1}H-^{13}C) HMBC NMR spectrum of 6a

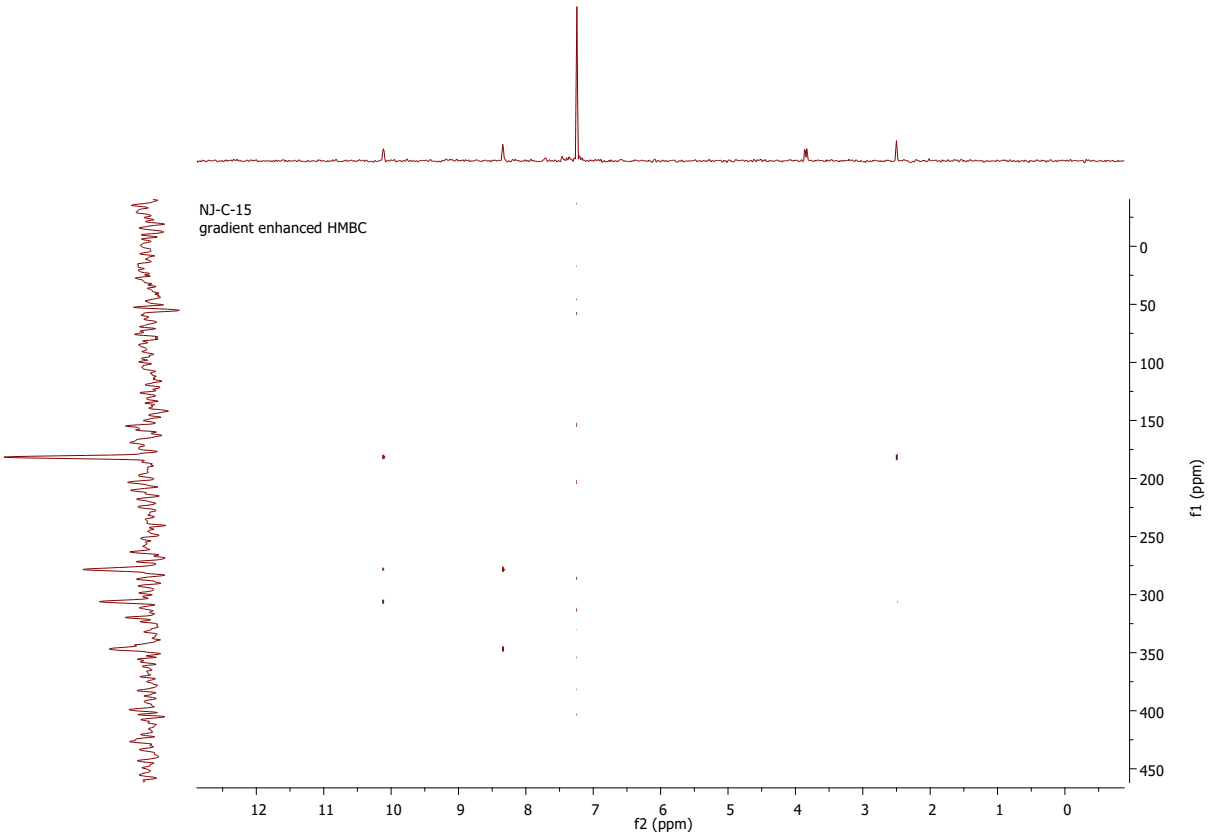

Figure S10. (^{1}H-^{15}N) HMBC NMR spectrum of 6a

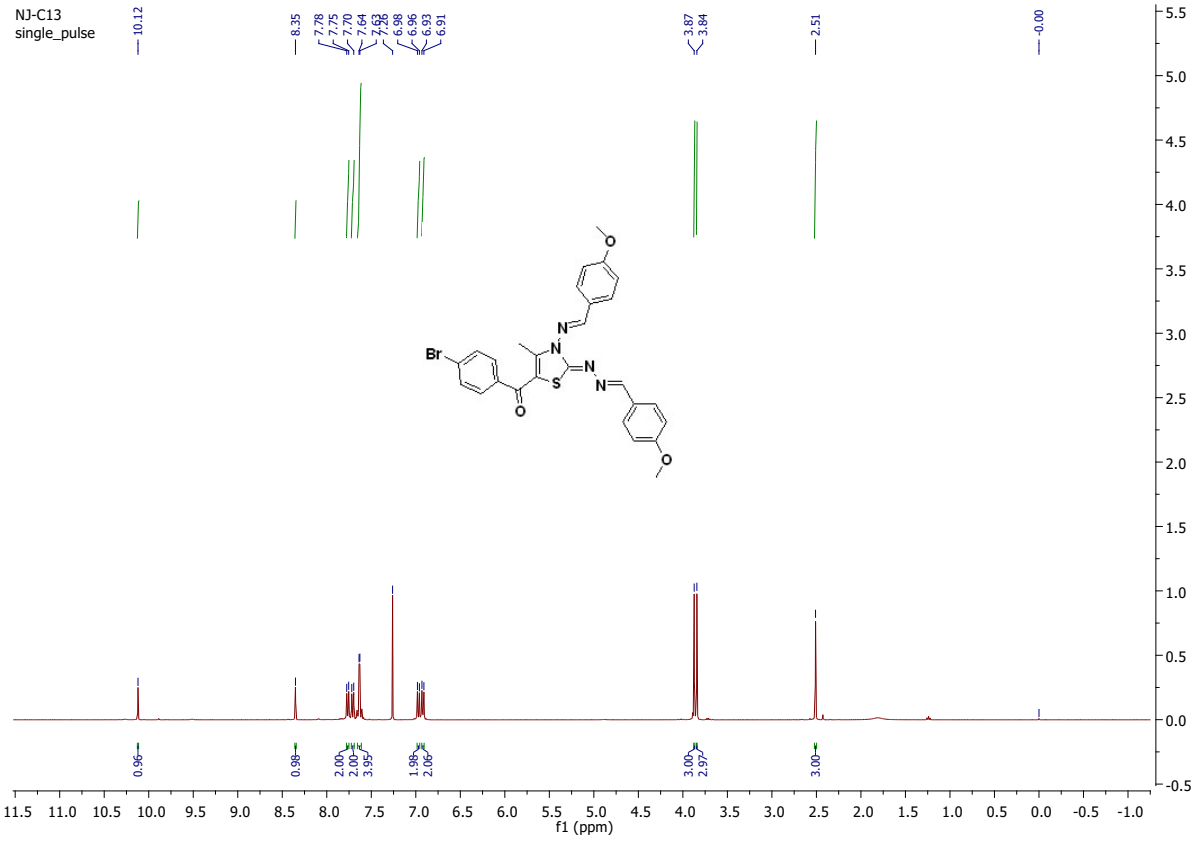

Figure S11. ^{1}H NMR spectrum of 6b

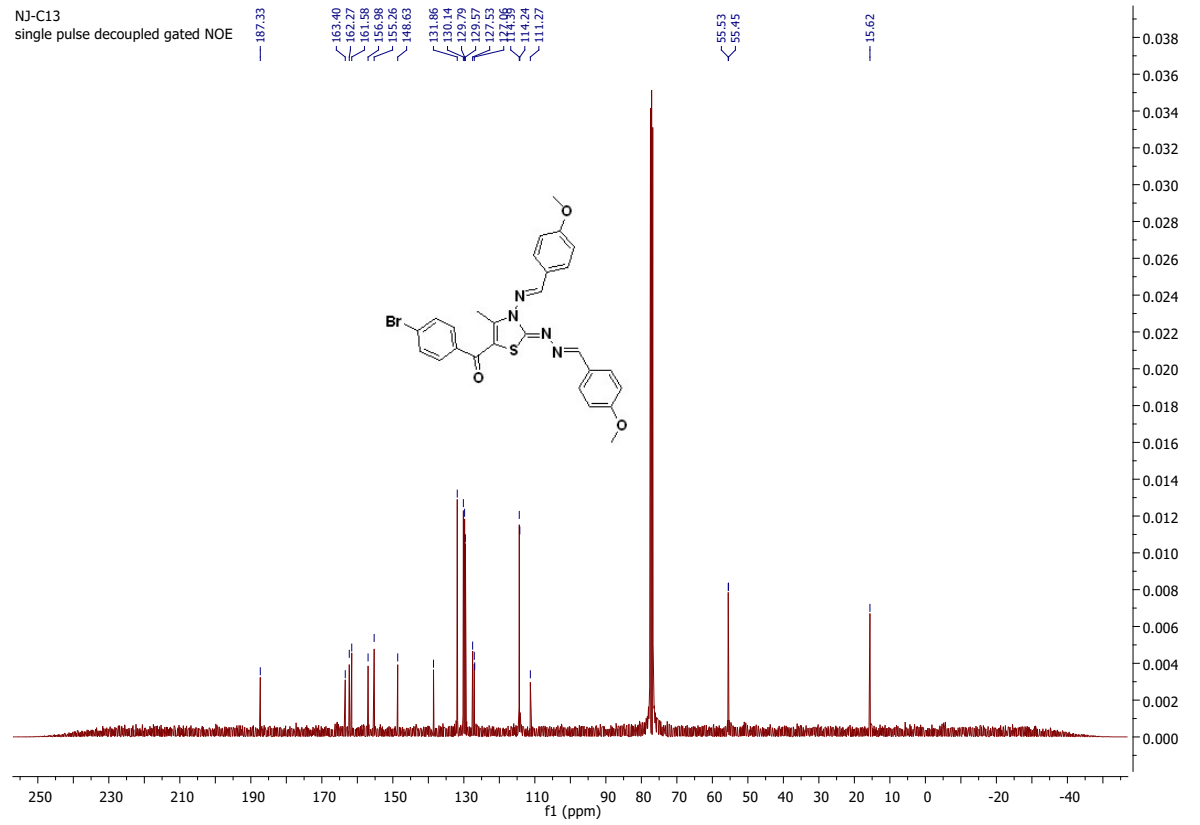

Figure S12. ^{13}C NMR spectrum of 6b

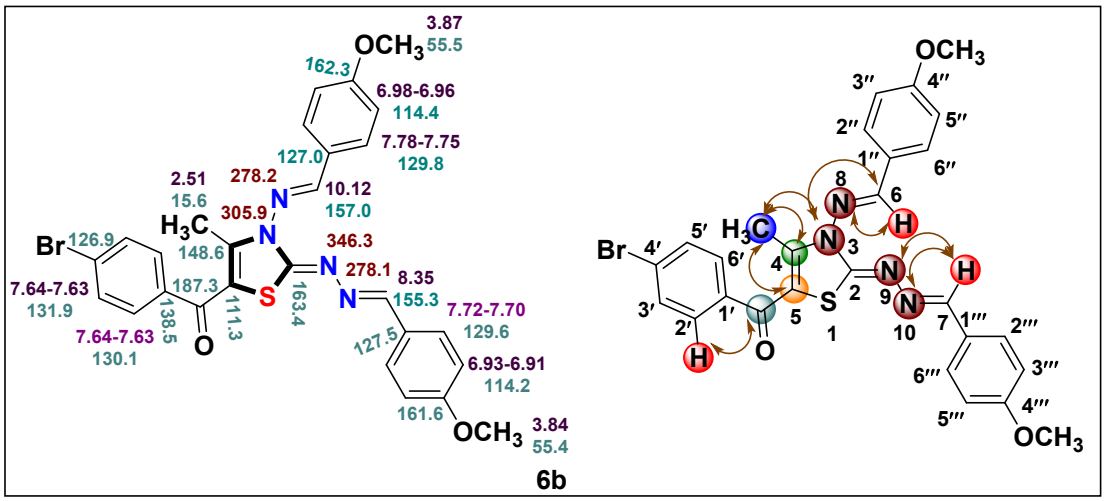

Table S3: 2D NMR correlation results for compound **6b**

Chemical shifts (δ in ppm)	gs-HSQC	gs-HMBC	Assignment
187.3	-	7.64-7.63 (H-2', 6')	CO
163.4	-	-	C-2
162.3	-	6.98-6.96 (H-3", 5") 3.87 (4"-OCH_3)	C-4"
161.6	-	6.93-6.91 (H-3"', 5"') 3.84 (4"'-OCH_3)	C-4"'
157.0	10.12 (H-6)	-	C-6
155.3	8.35 (H-7)	-	C-7
148.6	-	2.51 (4-CH_3)	C-4
138.5	-	7.64-7.63 (H-2', 6')	C-1'
131.9	7.64-7.63 (H-3', 5')	7.64-7.63 (H-2', 6')	C-3', 5'
130.1	7.64-7.63 (H-2', 6')	7.64-7.63 (H-3', 5')	C-2', 6'
129.8	7.78-7.75 (H-2", 6")	6.98-6.96 (H-3", 5")	C-2", 6"
129.6	7.72-7.70 (H-2"', 6"')	6.93-6.91 (H-3"', 5"')	C-2"', 6"'
127.5	-	7.72-7.70 (H-2"', 6"') 8.35 (H-7)	C-1"'
127.0	-	7.78-7.75 (H-2", 6") 10.12 (H-6)	C-1"
126.9	-	7.64-7.63 (H-2', 6')	C-4'
114.4	6.98-6.96 (H-3", 5")	7.78-7.75 (H-2", 6")	C-3", 5"
114.2	6.93-6.91 (H-3"', 5"')	7.72-7.70 (H-2"', 6"')	C-3"', 5"'
111.3	-	2.51 (4-CH_3)	C-5
55.5	3.87 (4"-OCH_3)	-	4"-OCH_3
55.4	3.84 (4"'-OCH_3)	-	4"'-OCH_3
15.6	2.51 (4-CH_3)	-	4-CH_3
346.3	-	8.35 (H-7)	9-N
305.9	-	10.12 (H-6) 2.51 (4-CH_3)	3-N
278.2	-	10.12 (H-6)	8-N
278.1	-	8.35 (H-7)	10-N

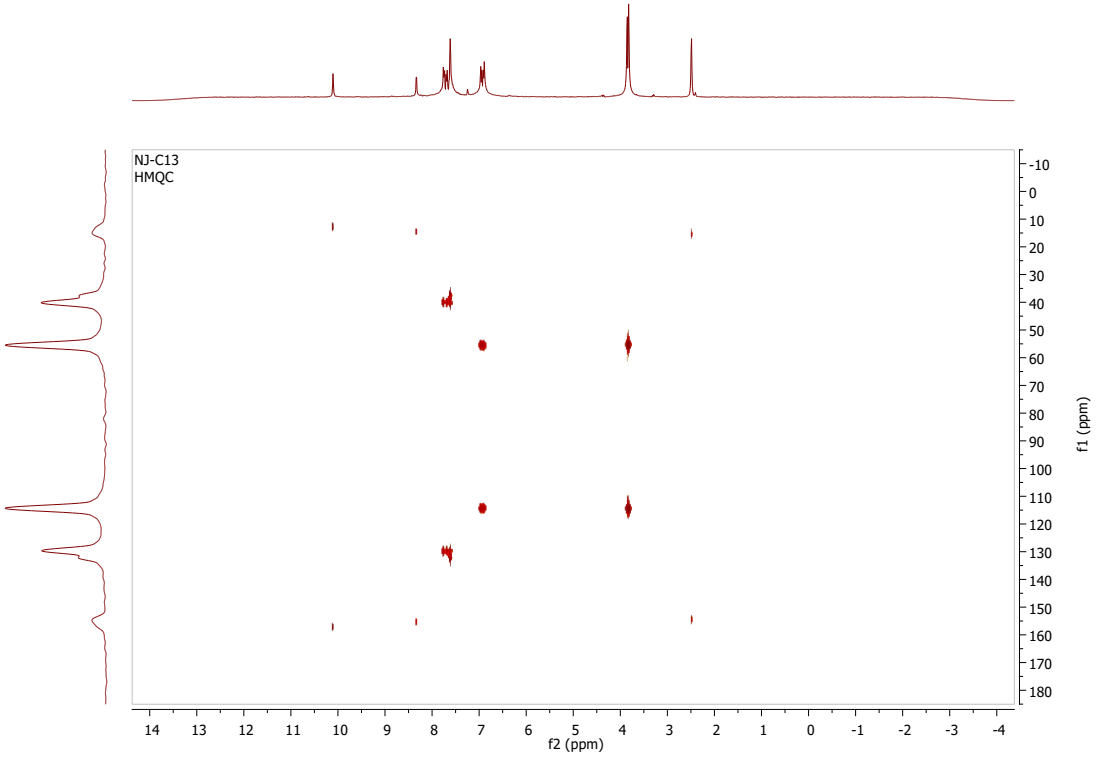

Figure S13. (^{1}H-^{13}C) HMQC NMR spectrum of 6b

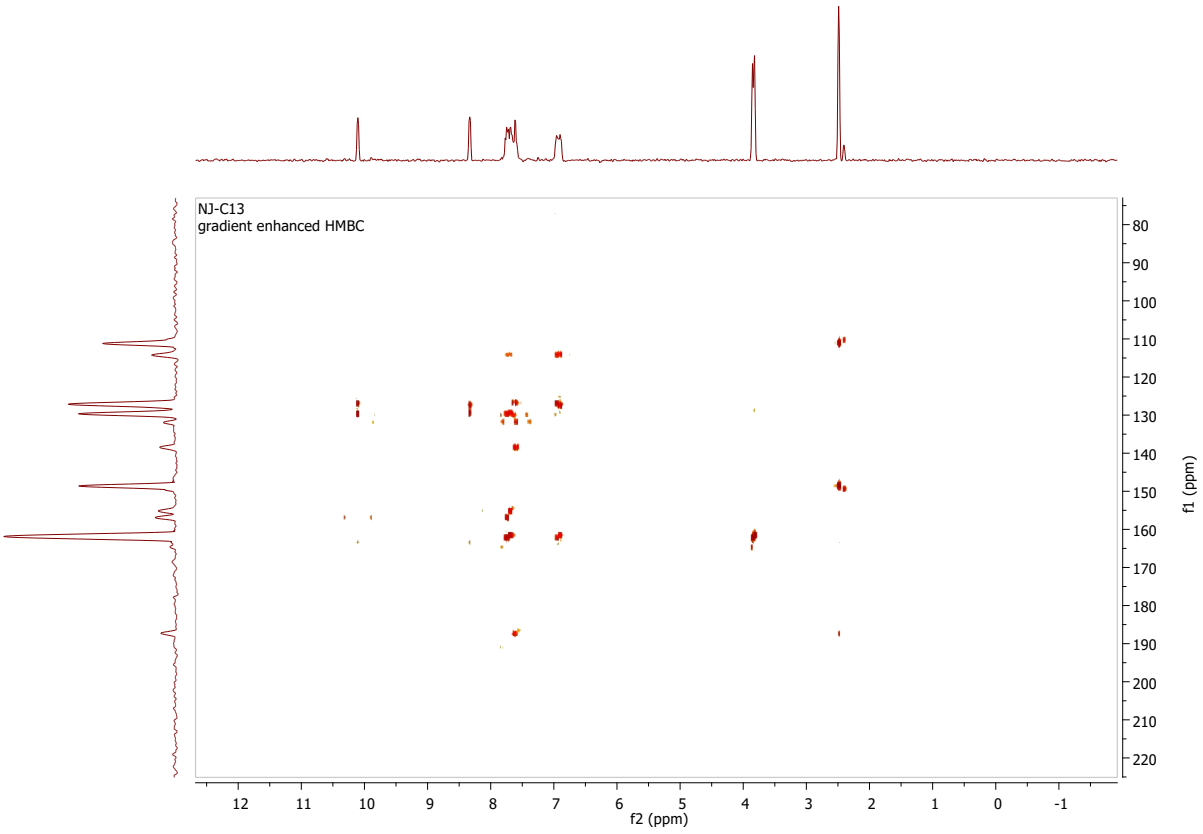

Figure S14. (^{1}H-^{13}C) HMBC NMR spectrum of 6b

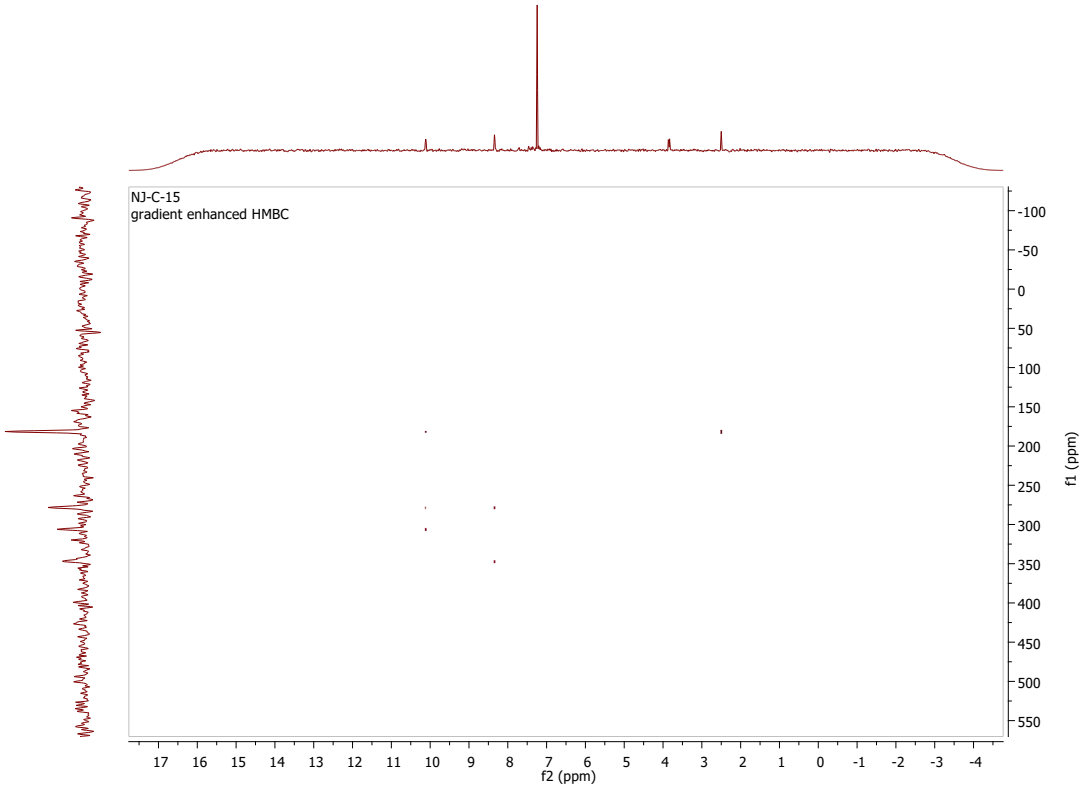

Figure S15. (^{1}H-^{15}N) HMBC NMR spectrum of 6b

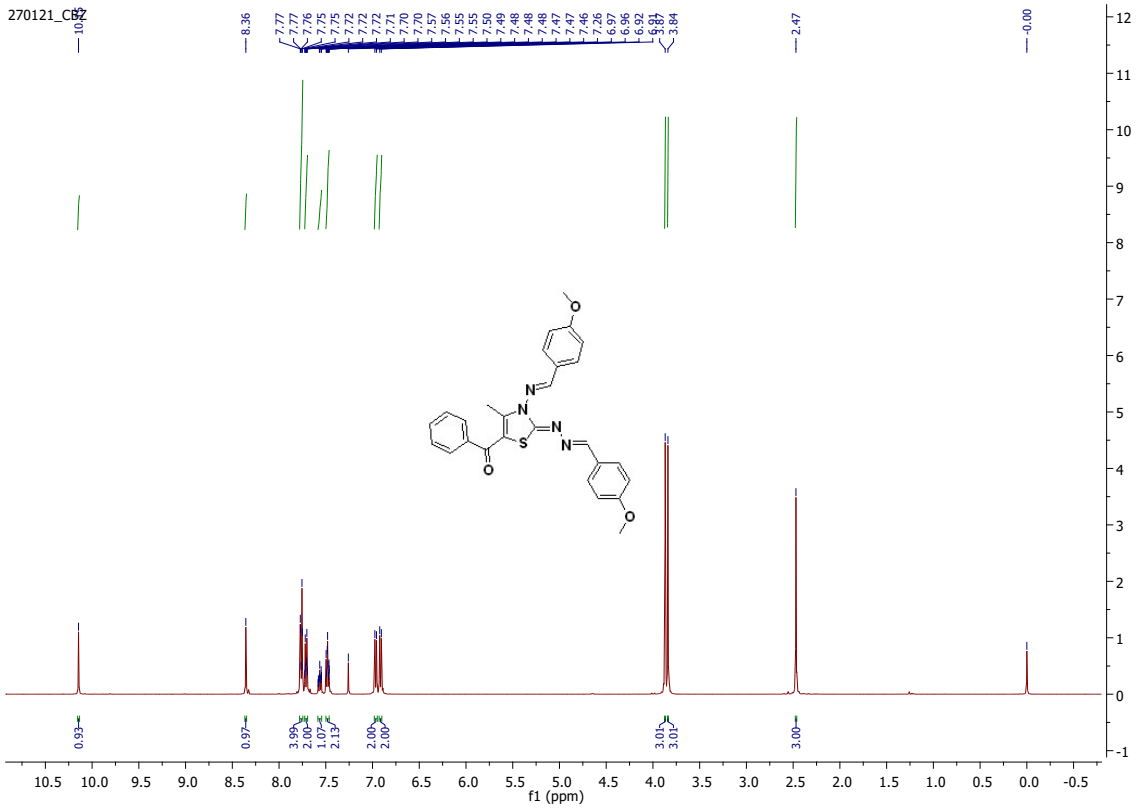

Figure S16. ^{1}H NMR spectrum of 6c

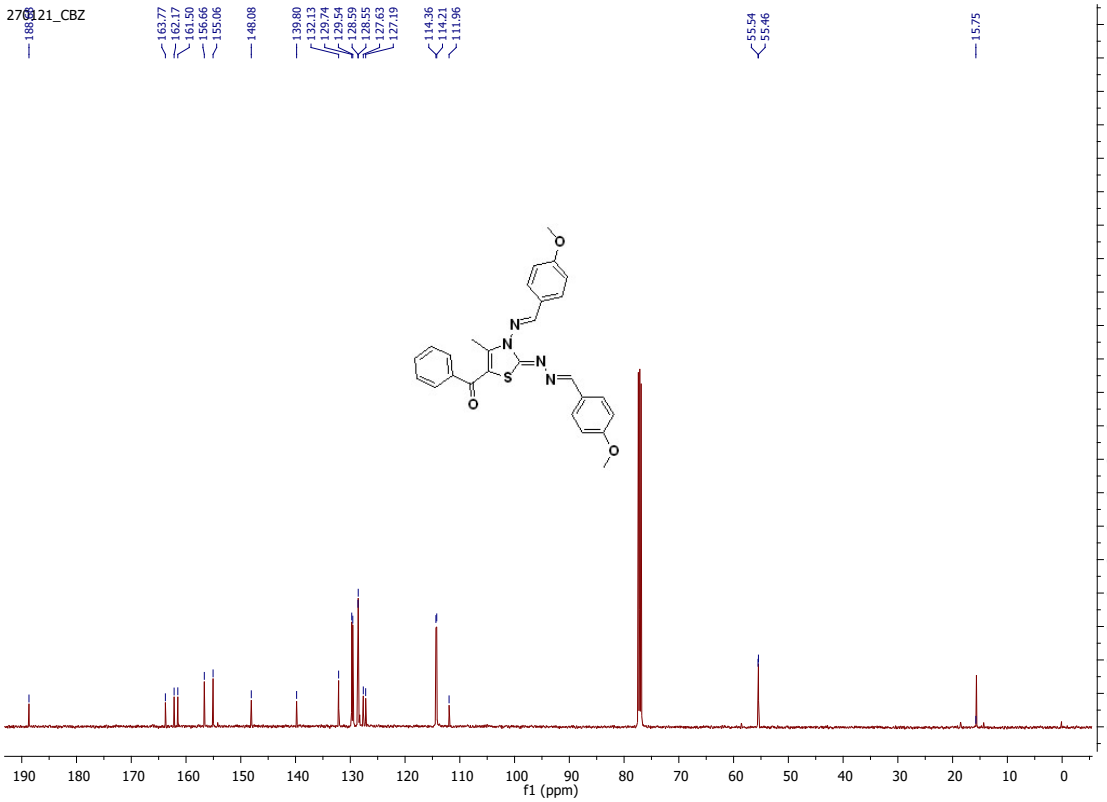

Figure S17. ^{13}C NMR spectrum of 6c

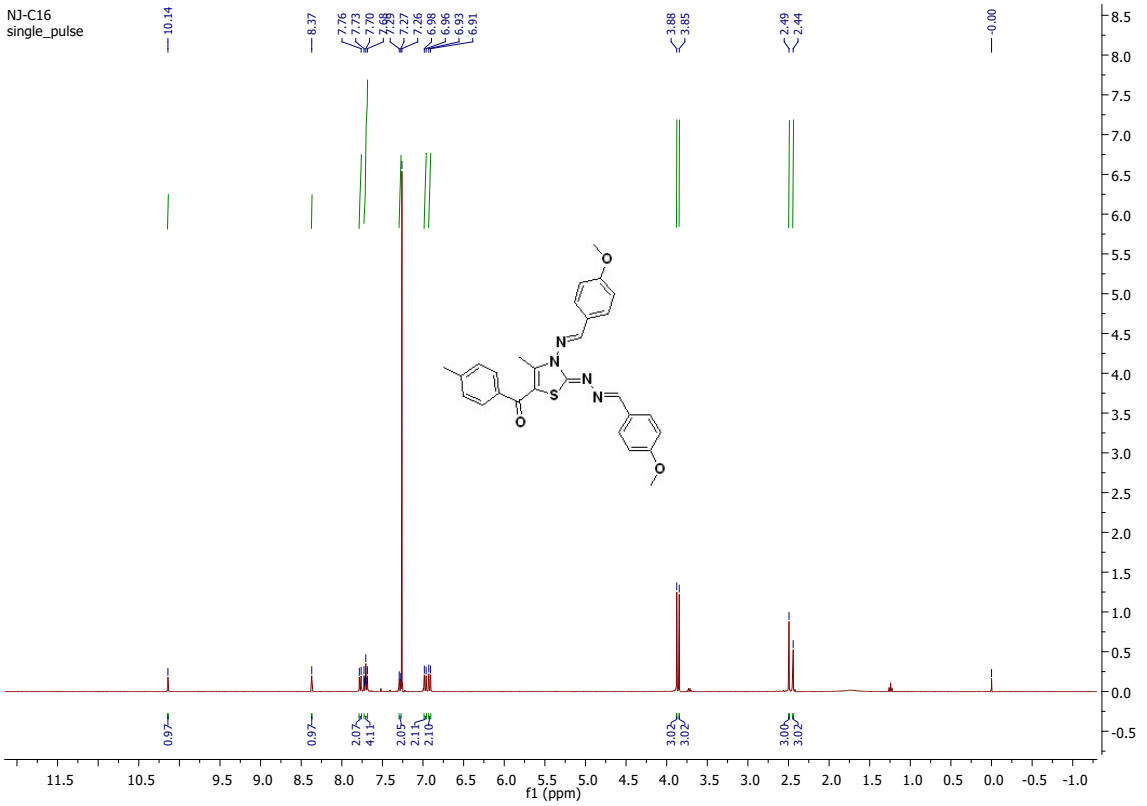

Figure S18. ^{1}H NMR spectrum of 6d

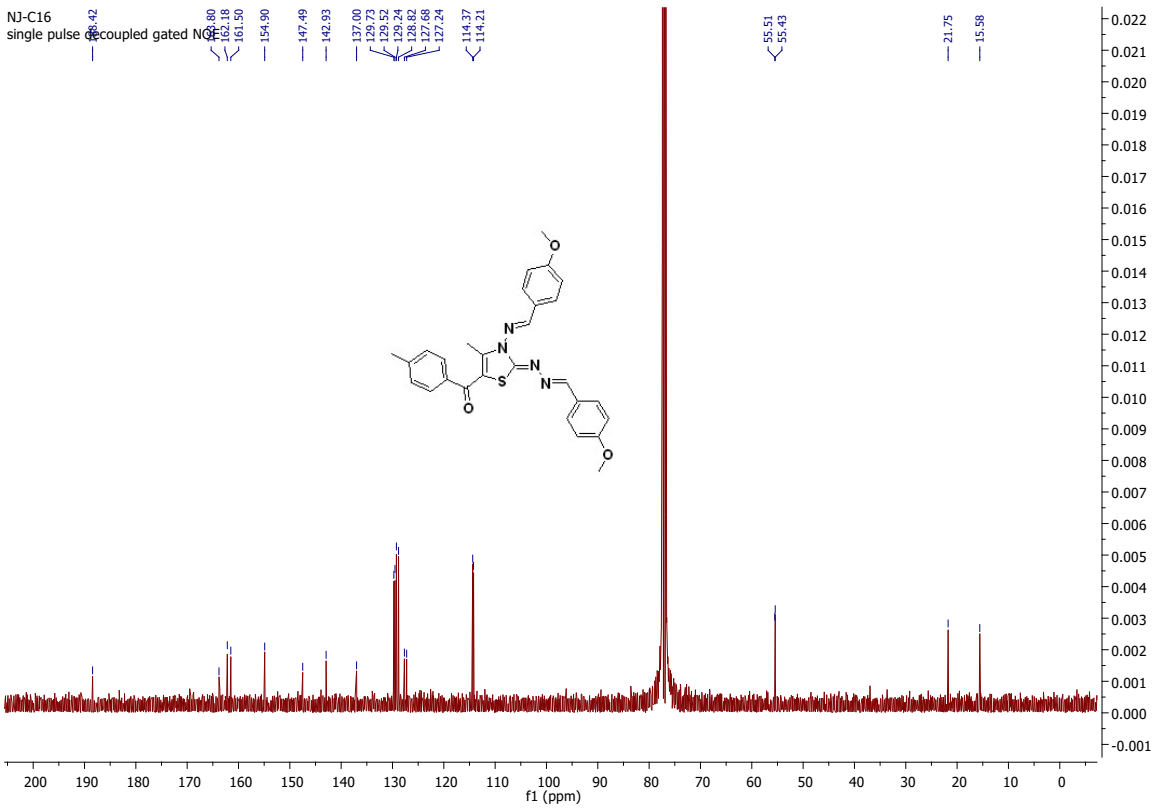

Figure S19. ^{13}C NMR spectrum of 6d

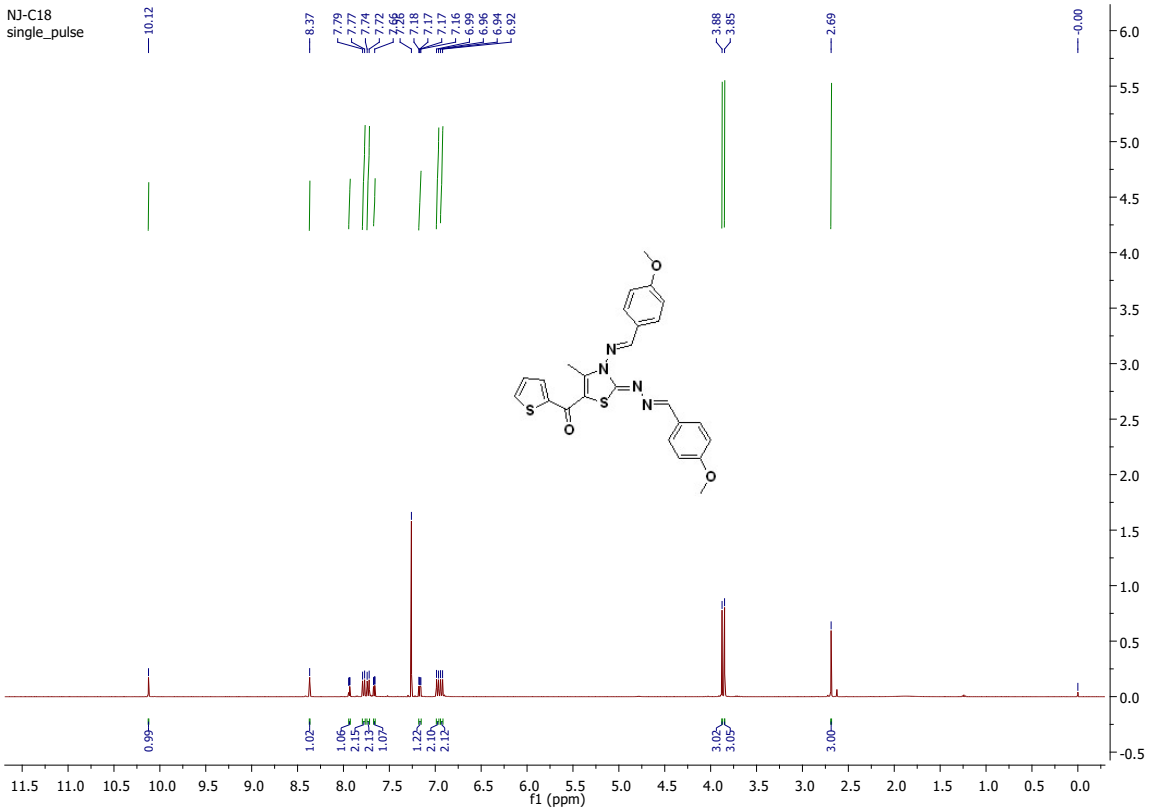

Figure S20. ^{1}H NMR spectrum of 6e

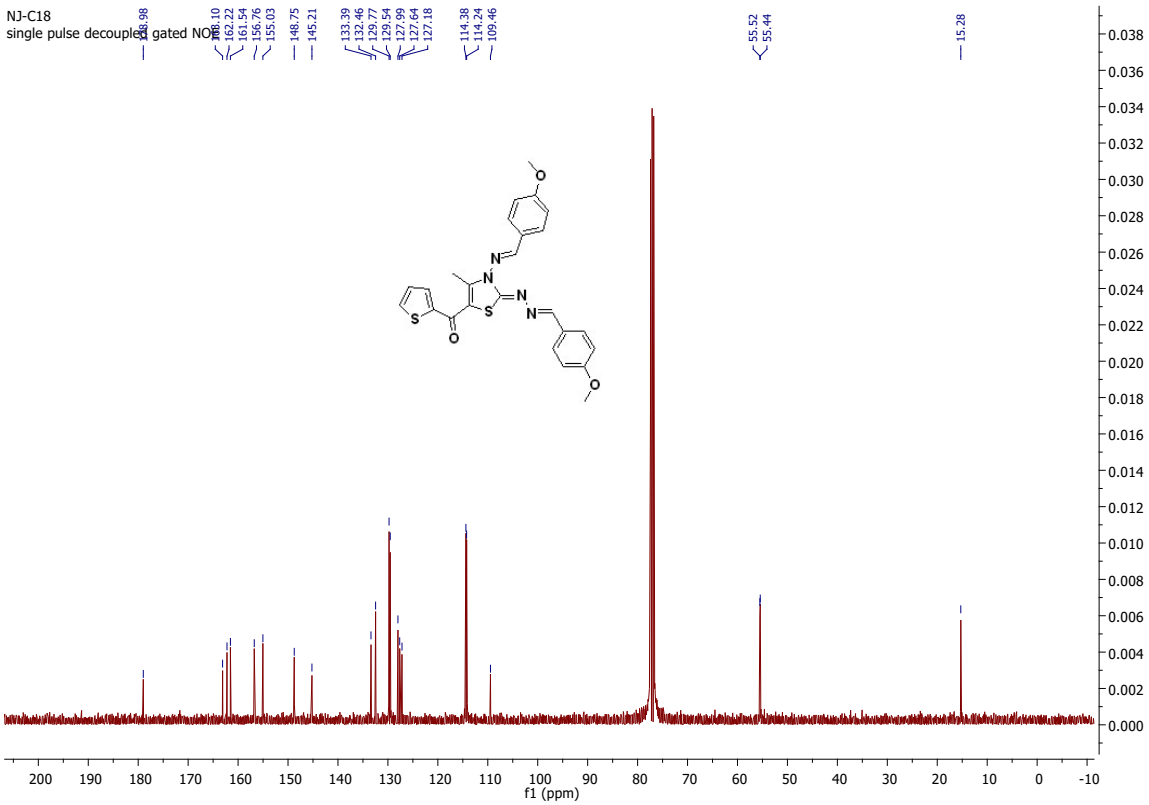

Figure S21. ^{13}C NMR spectrum of 6e

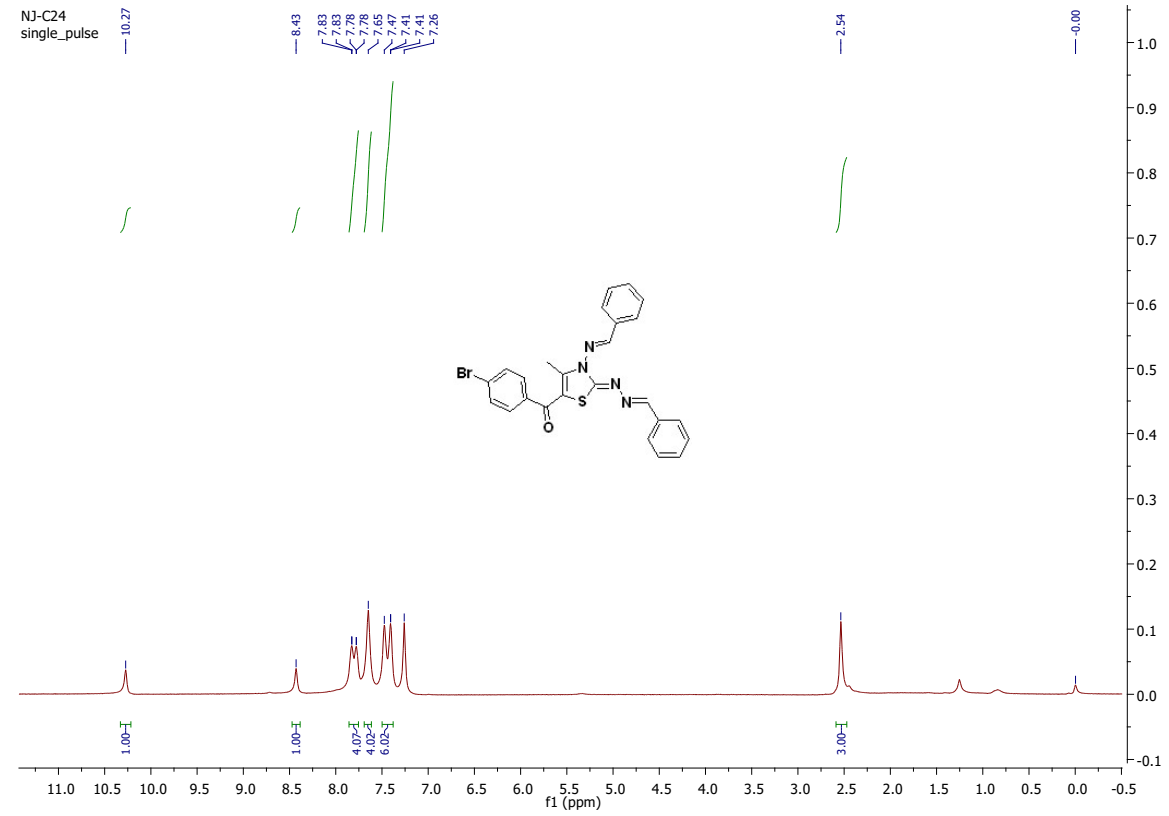

Figure S22. ^{1}H NMR spectrum of 6f

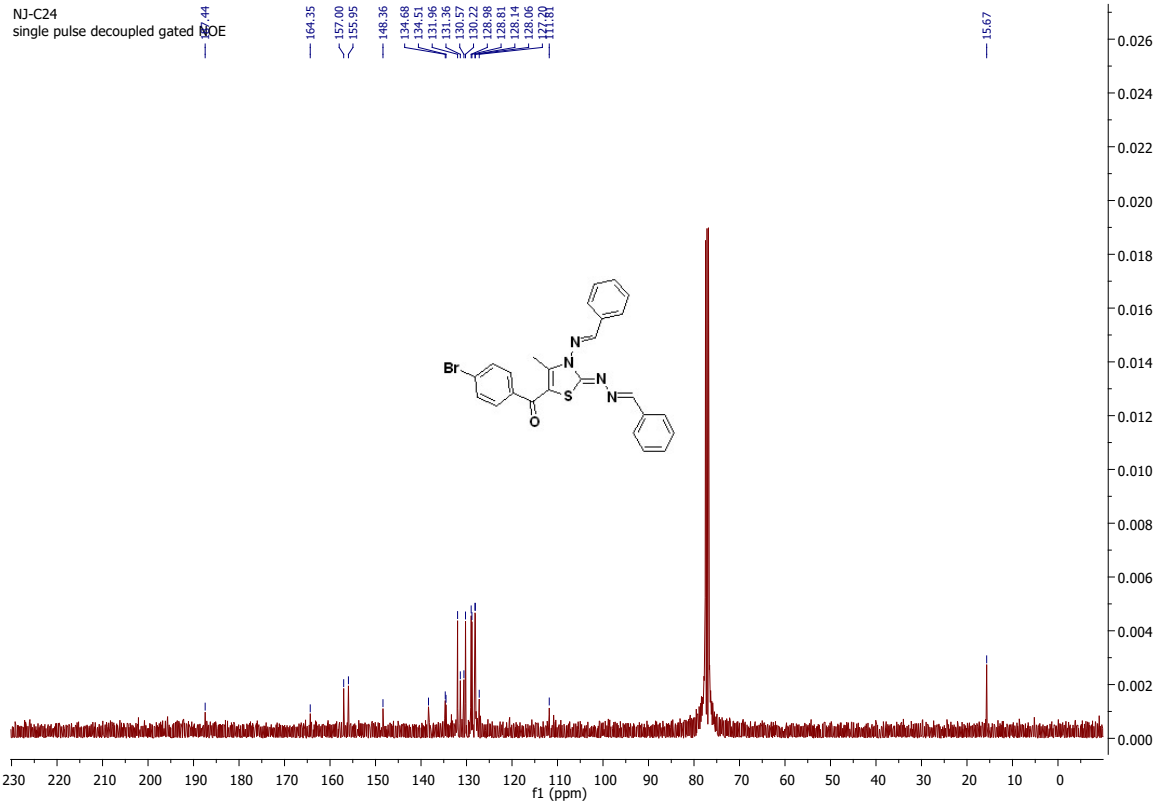

Figure S23. ^{13}C NMR spectrum of 6f

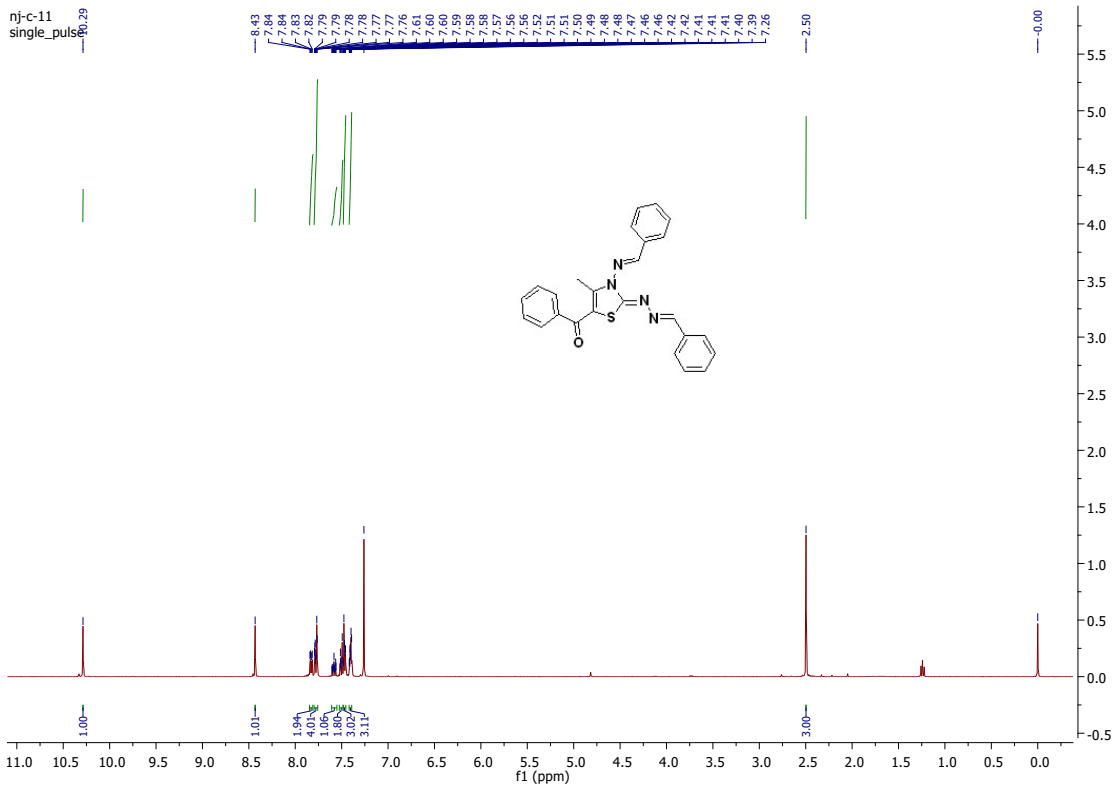

Figure S24. ^{1}H NMR spectrum of 6g

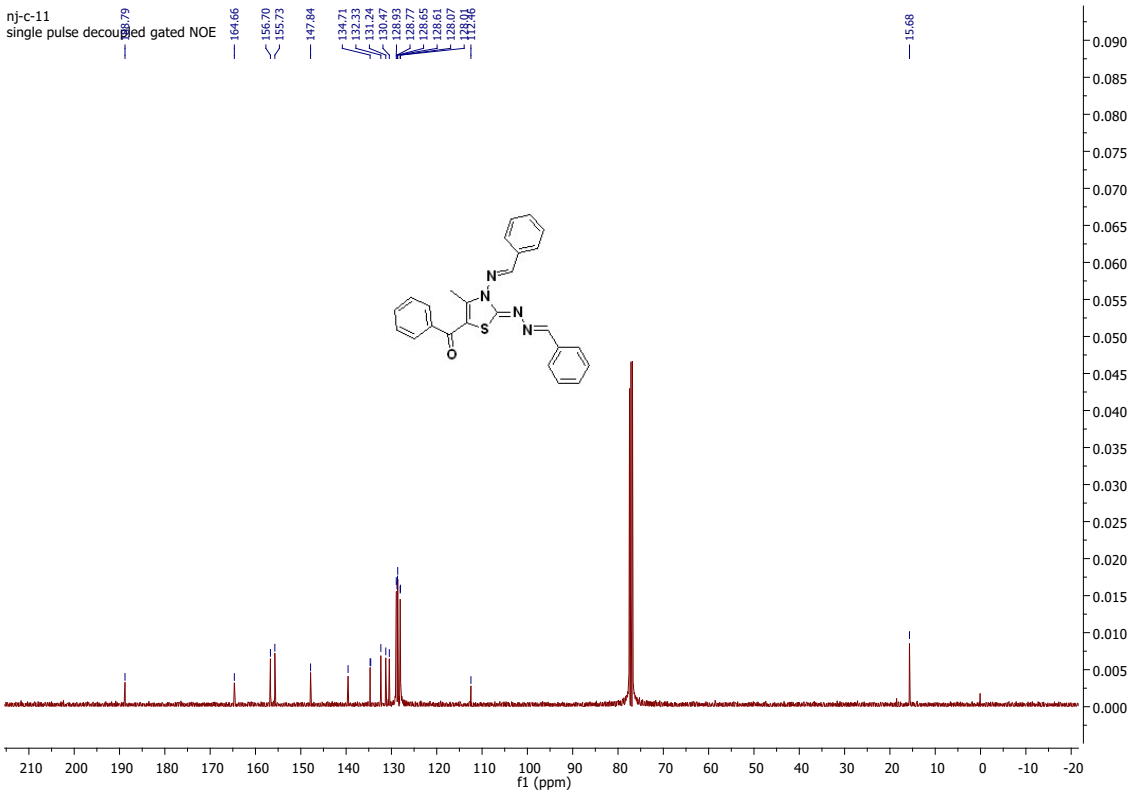

Figure S25. ^{13}C NMR spectrum of 6g

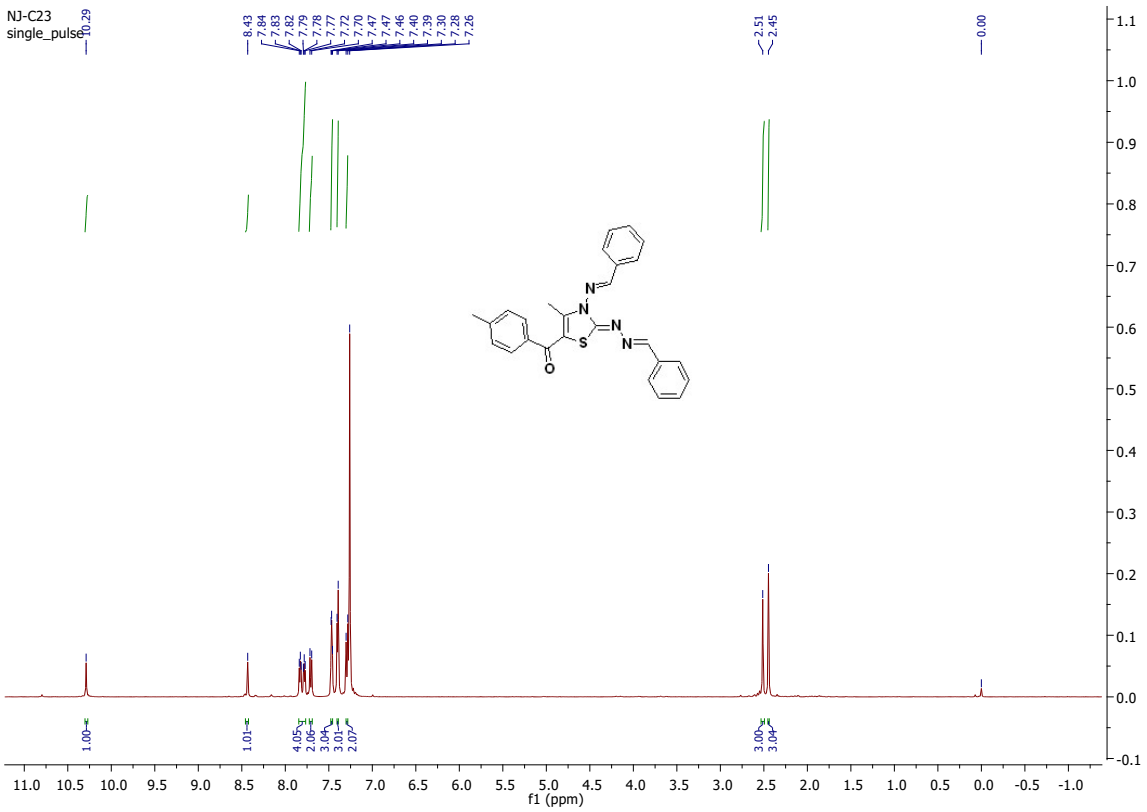

Figure S26. ^{1}H NMR spectrum of 6h

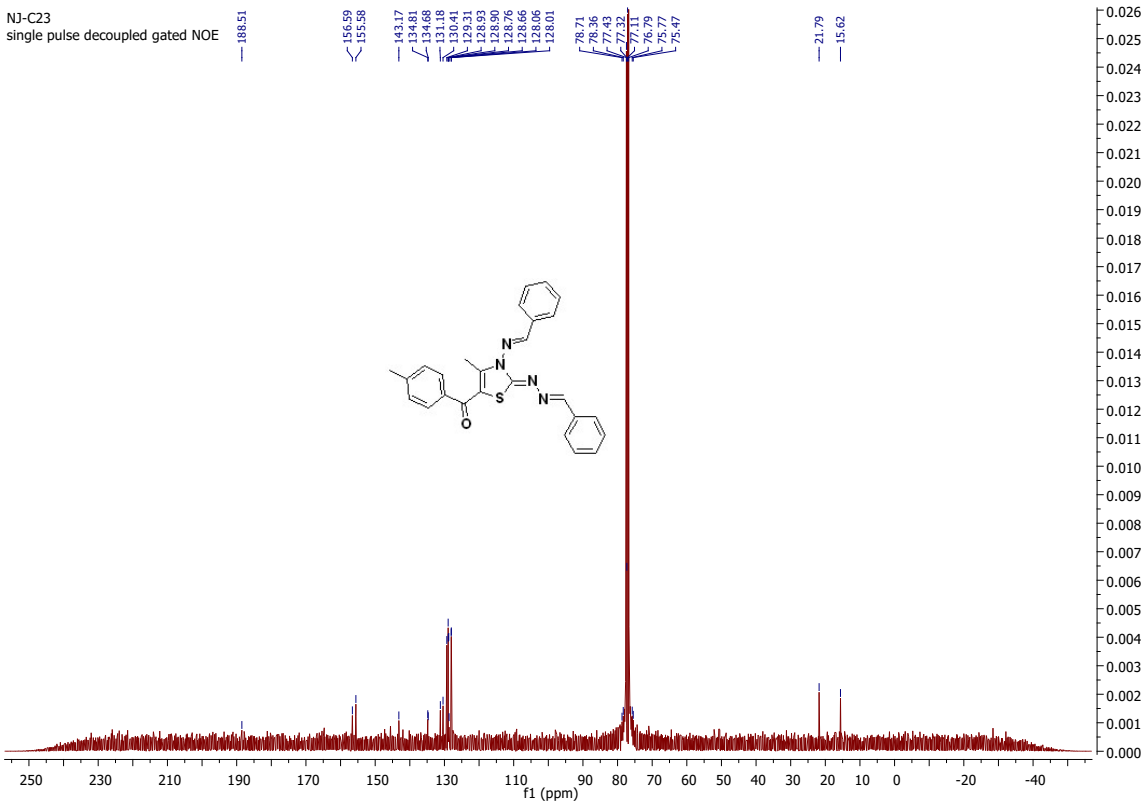

Figure S27. ^{13}C NMR spectrum of 6h

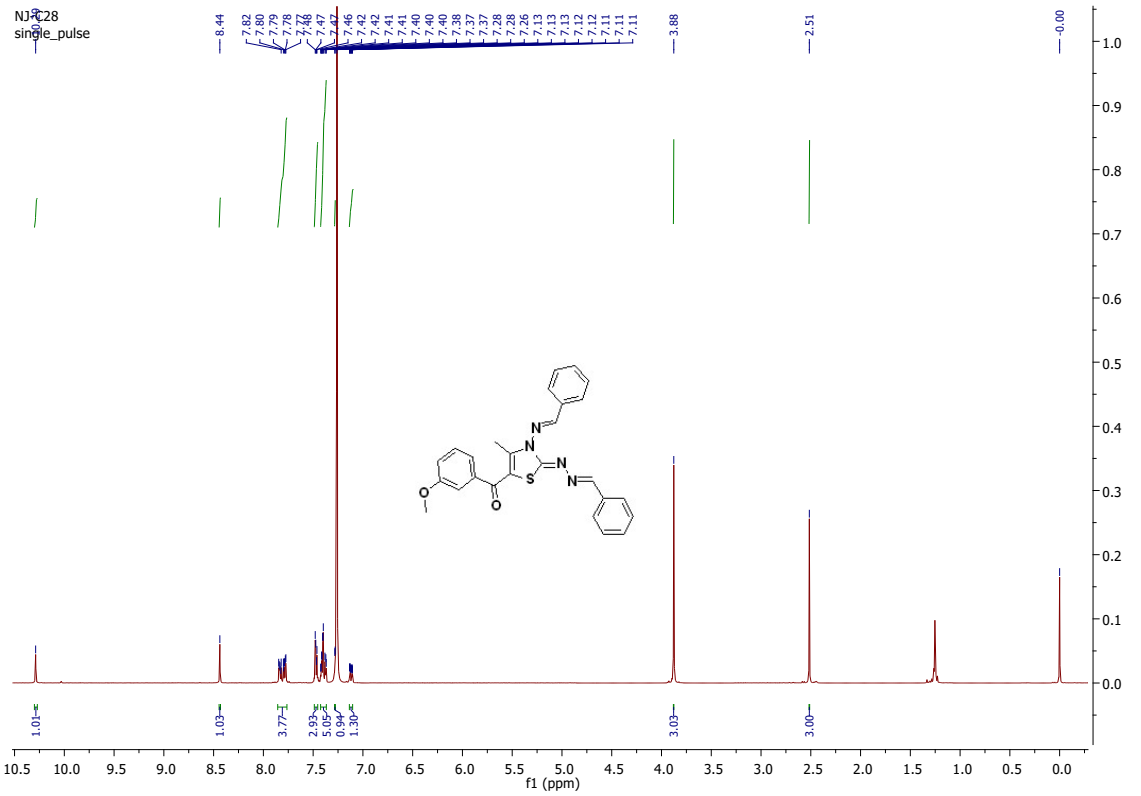

Figure S28. ^{1}H NMR spectrum of 6i

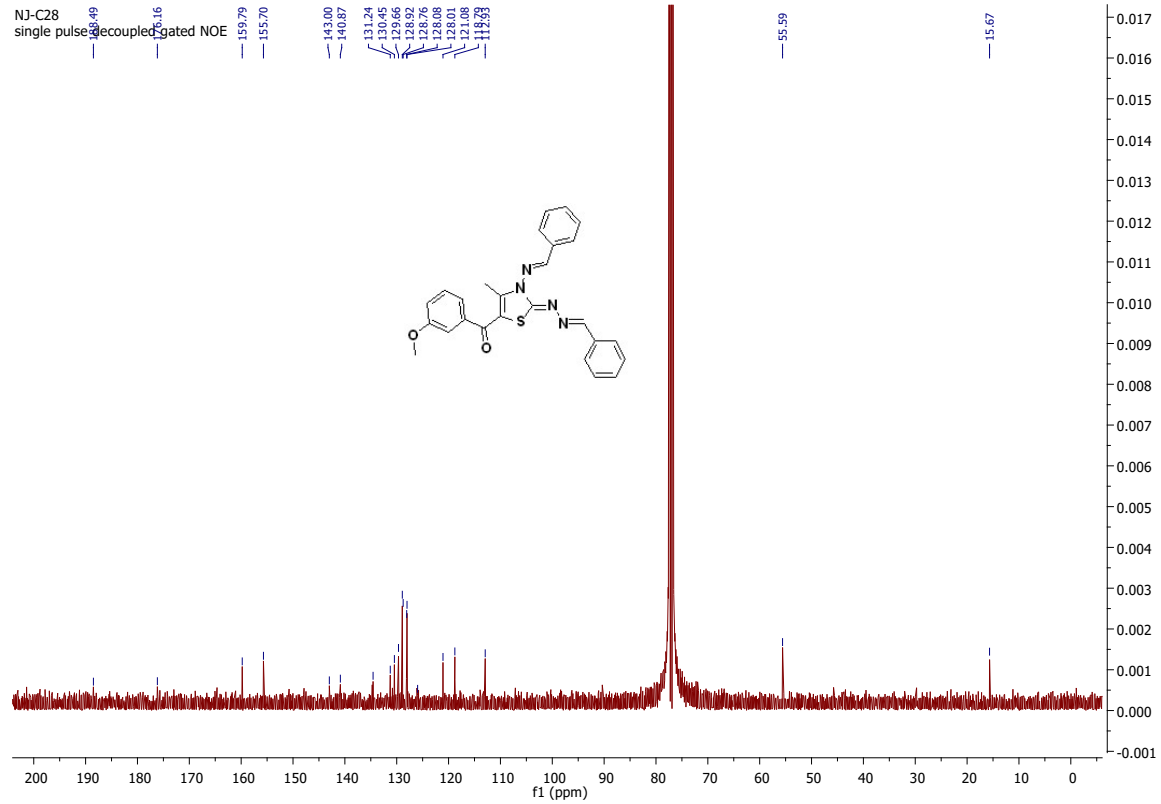

Figure S29. ^{13}C NMR spectrum of 6i

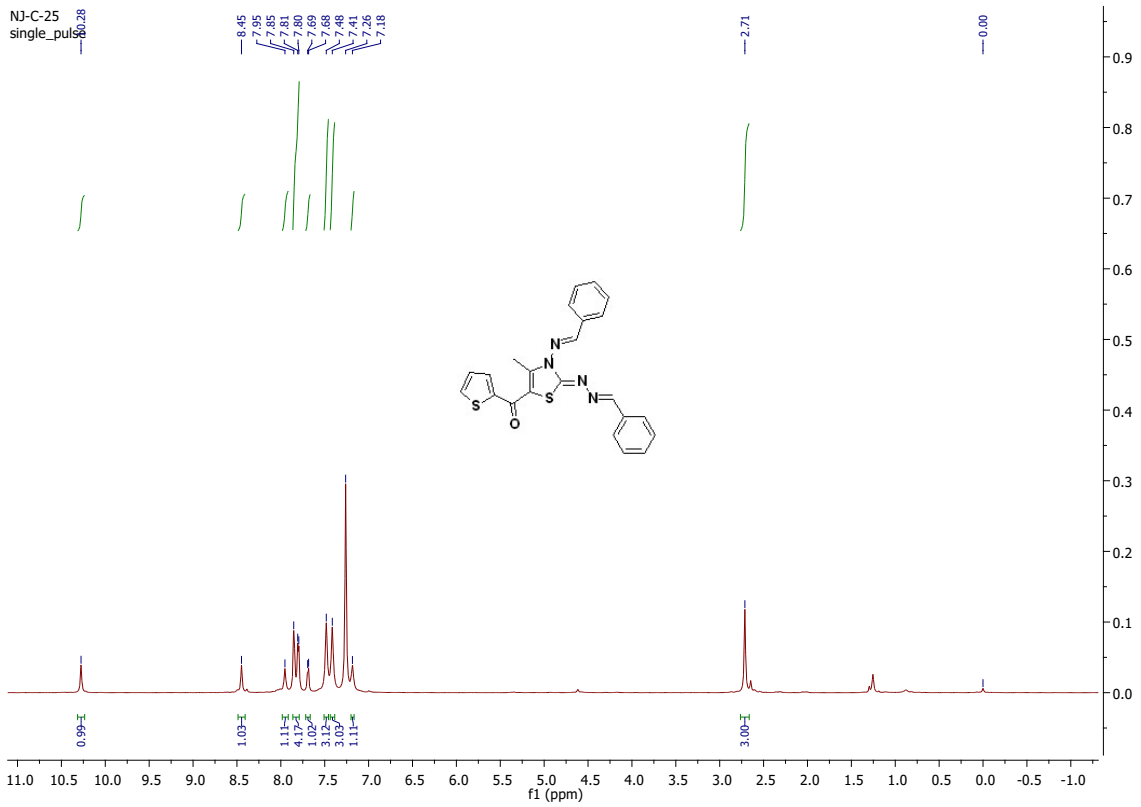

Figure S30. ^{1}H NMR spectrum of 6j

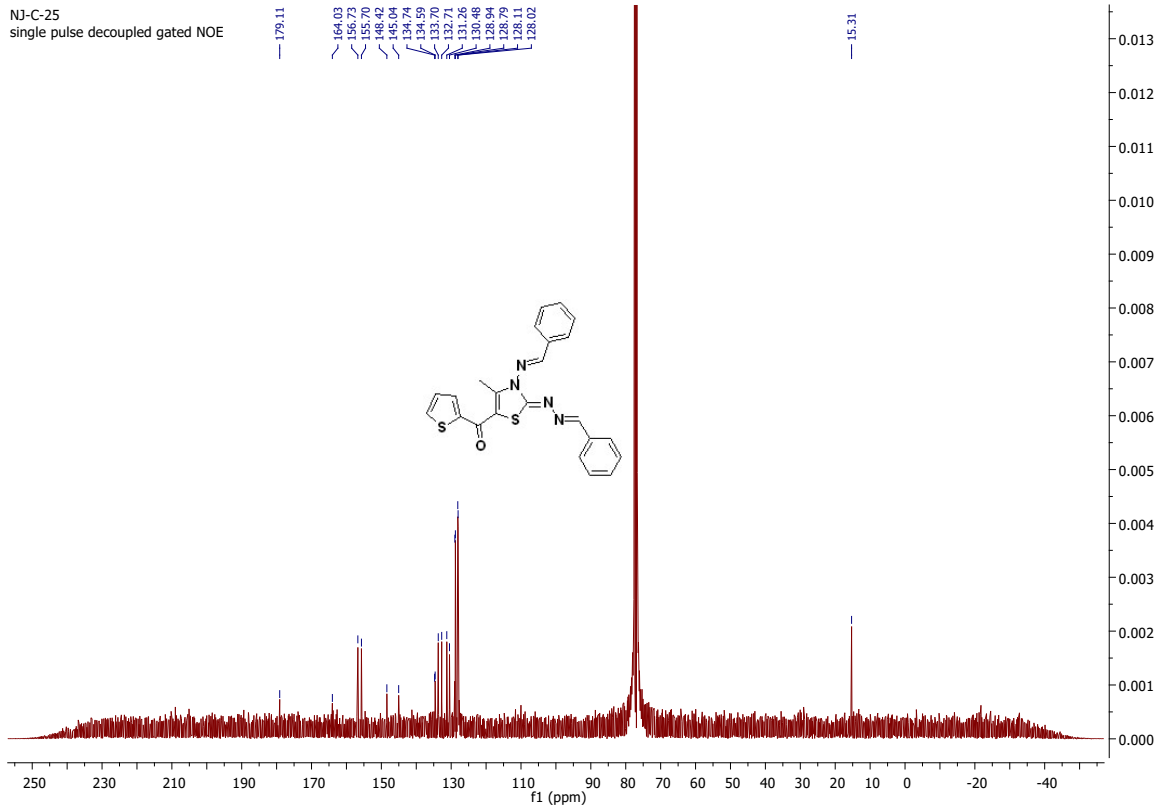

Figure S31. ^{13}C NMR spectrum of 6j

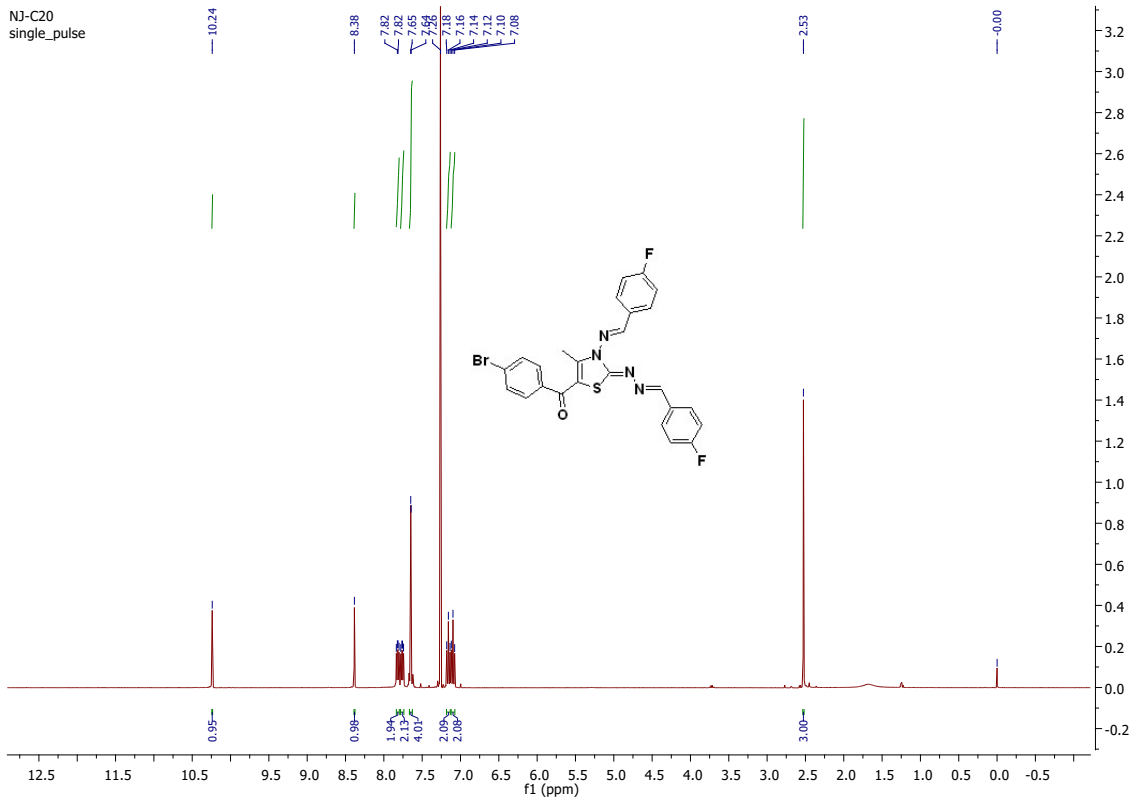

Figure S32. ^{1}H NMR spectrum of 6k

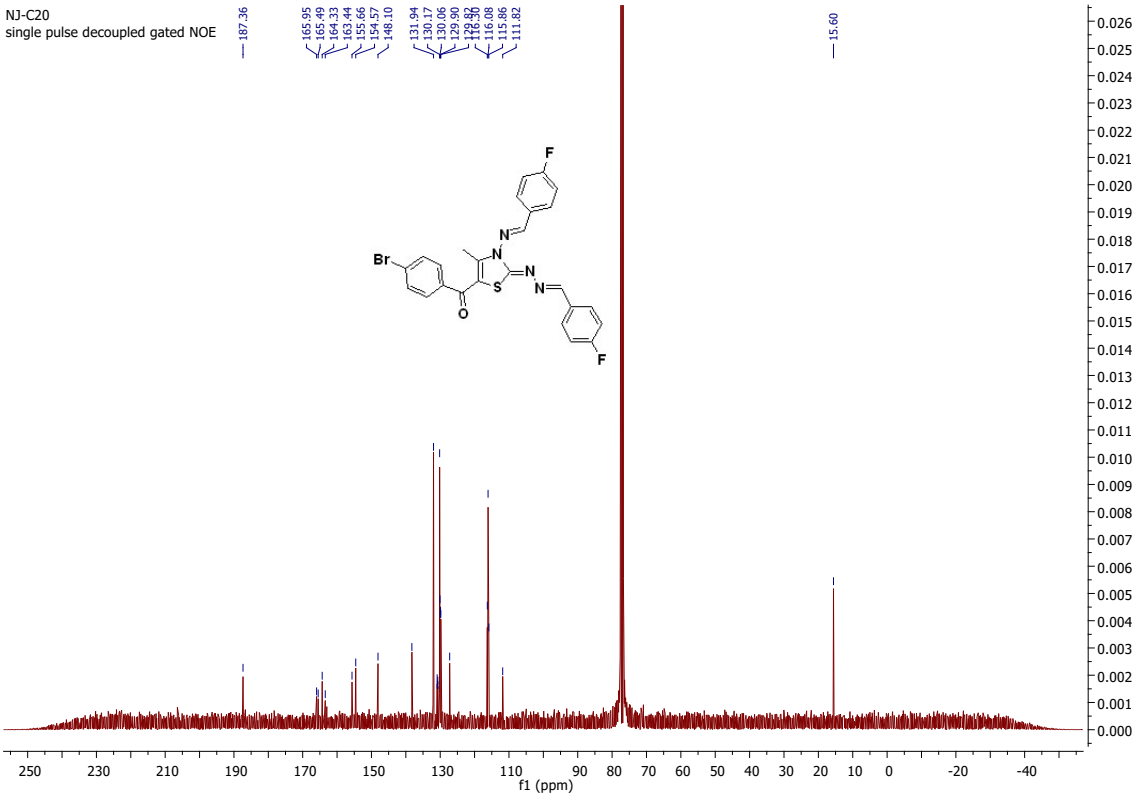

Figure S33. ^{13}C NMR spectrum of 6k

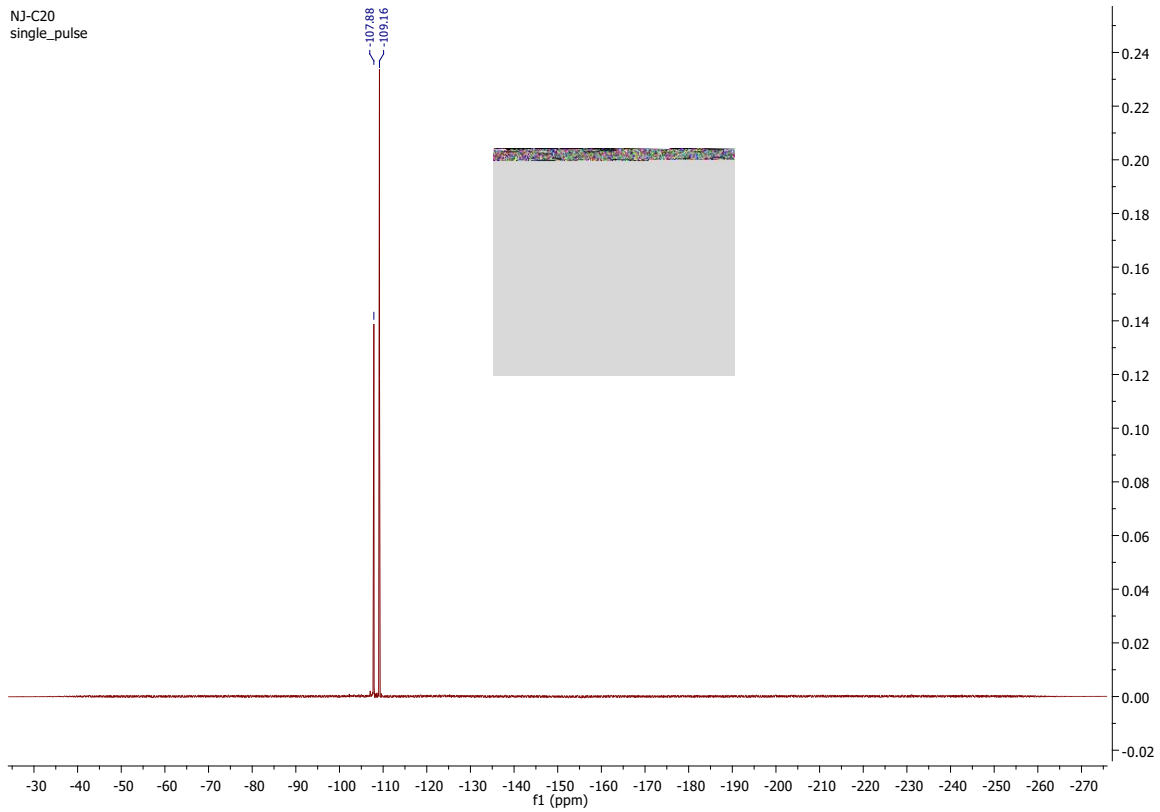

Figure S34. ^{19}F NMR spectrum of 6k

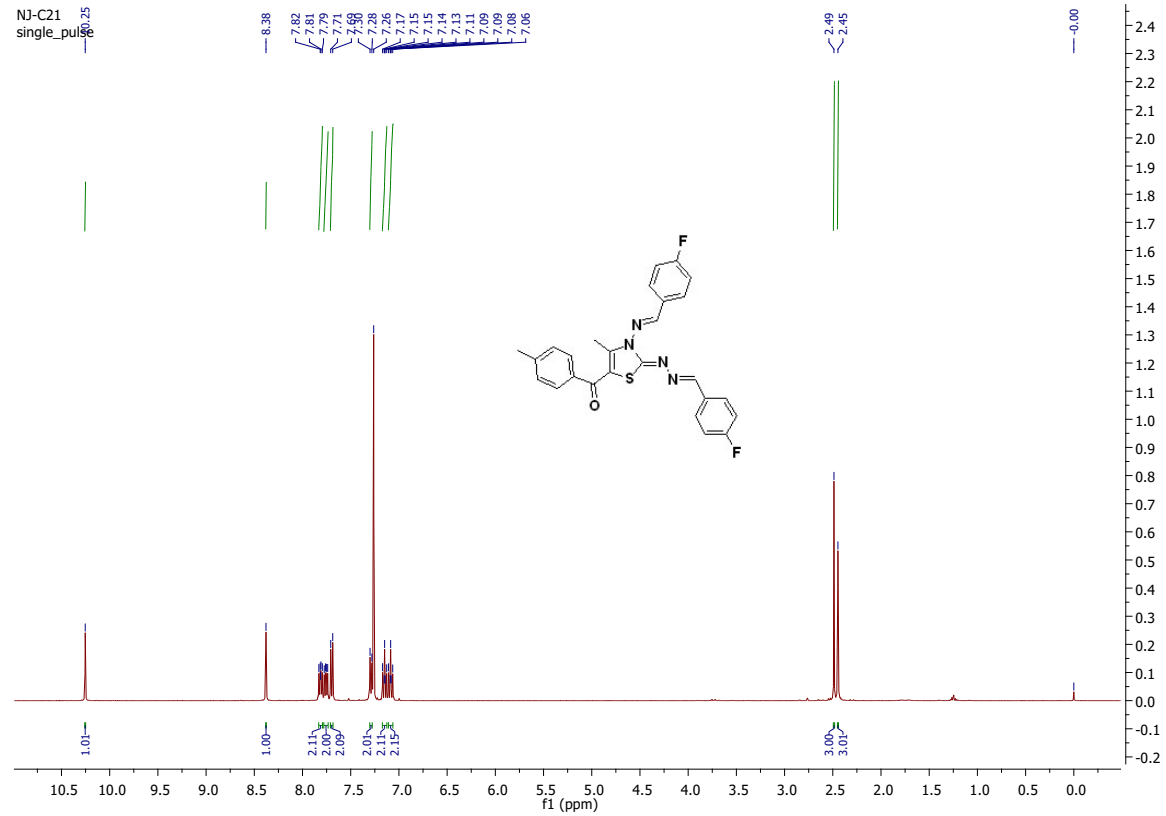

Figure S35. ^{1}H NMR spectrum of 6l

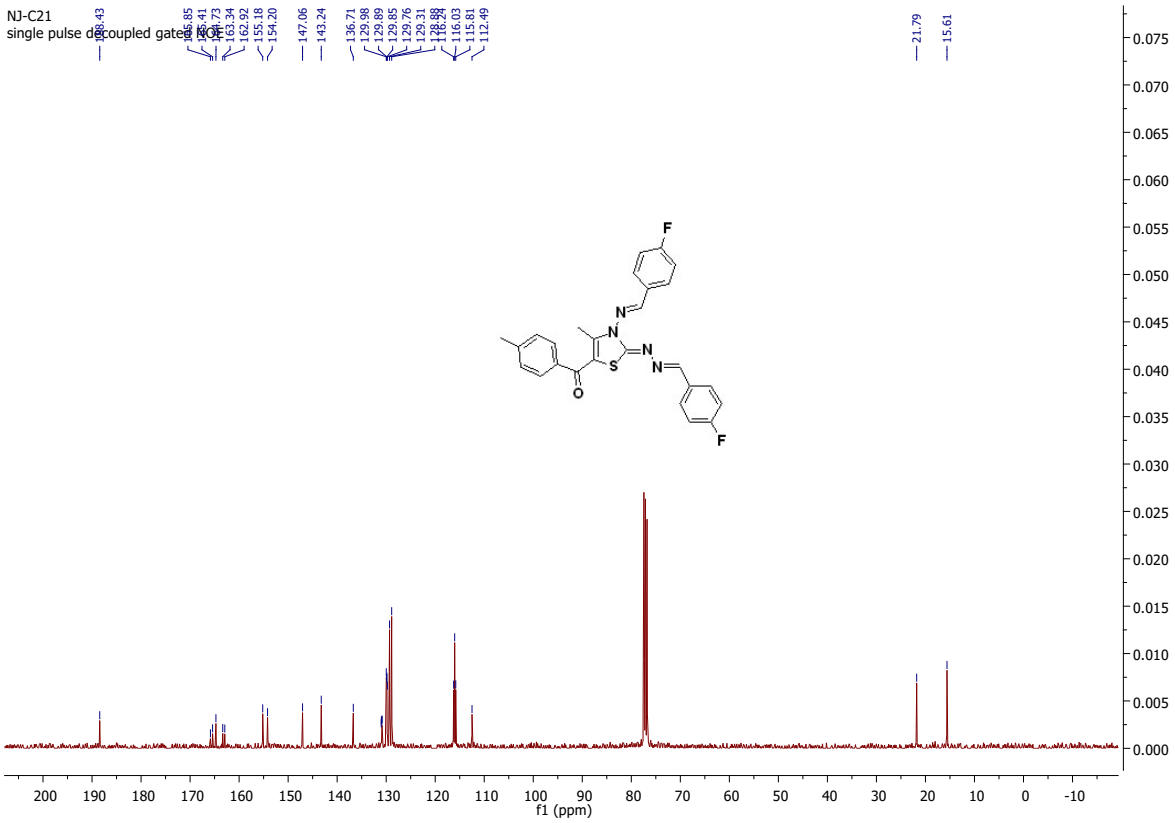

Figure S36. ^{13}C NMR spectrum of 6l

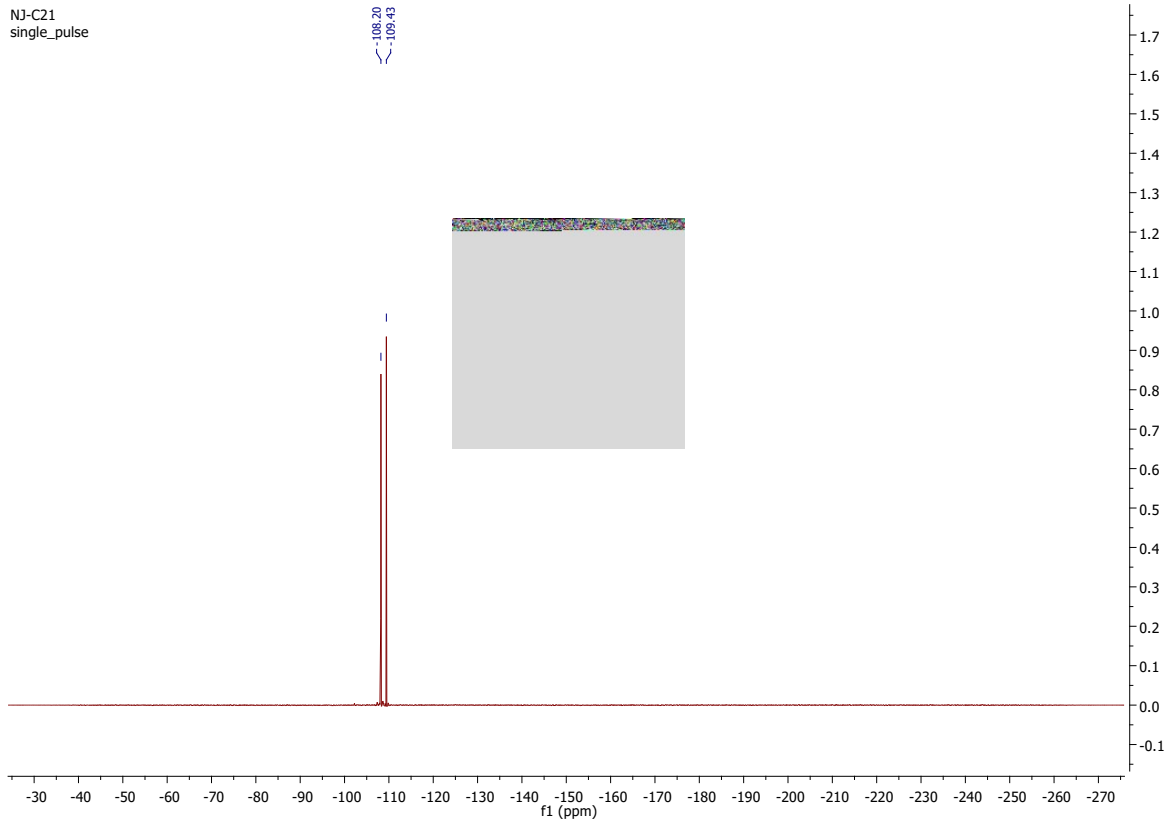

Figure S37. ^{19}F NMR spectrum of 6l

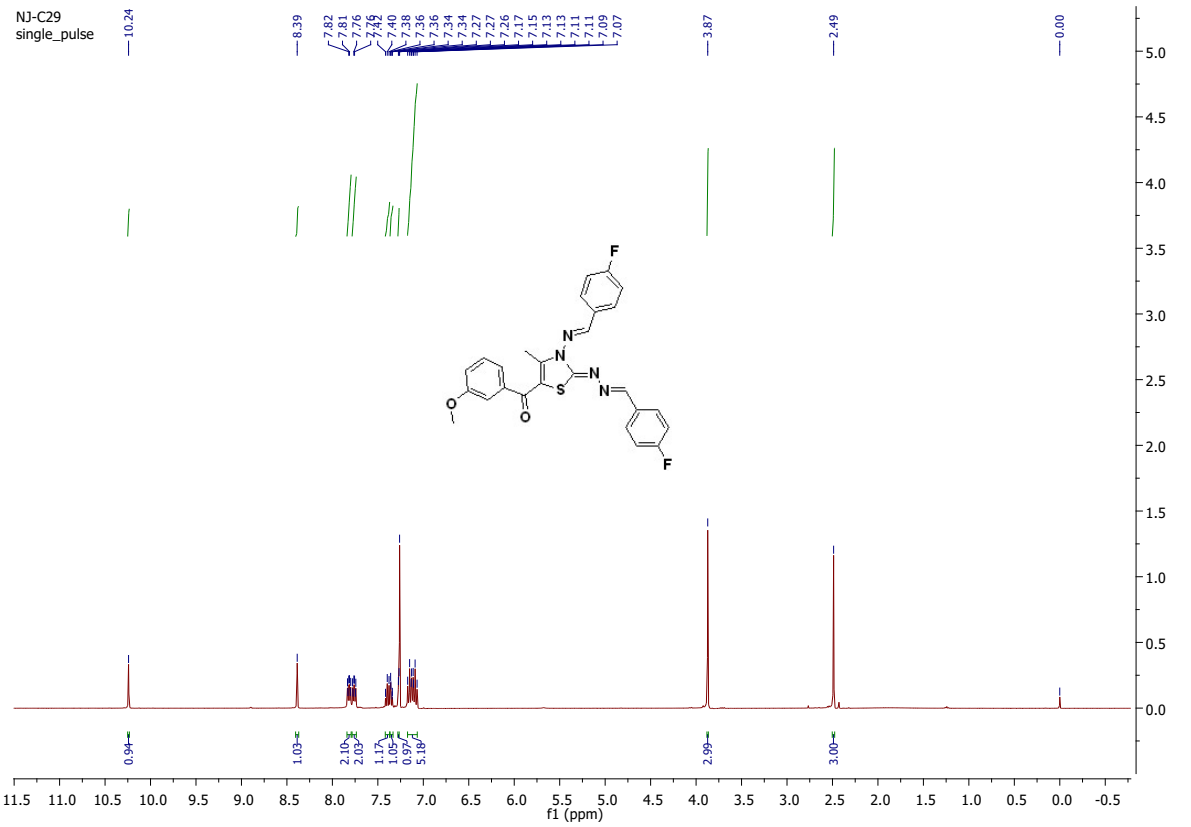

Figure S38. ^{1}H NMR spectrum of 6m

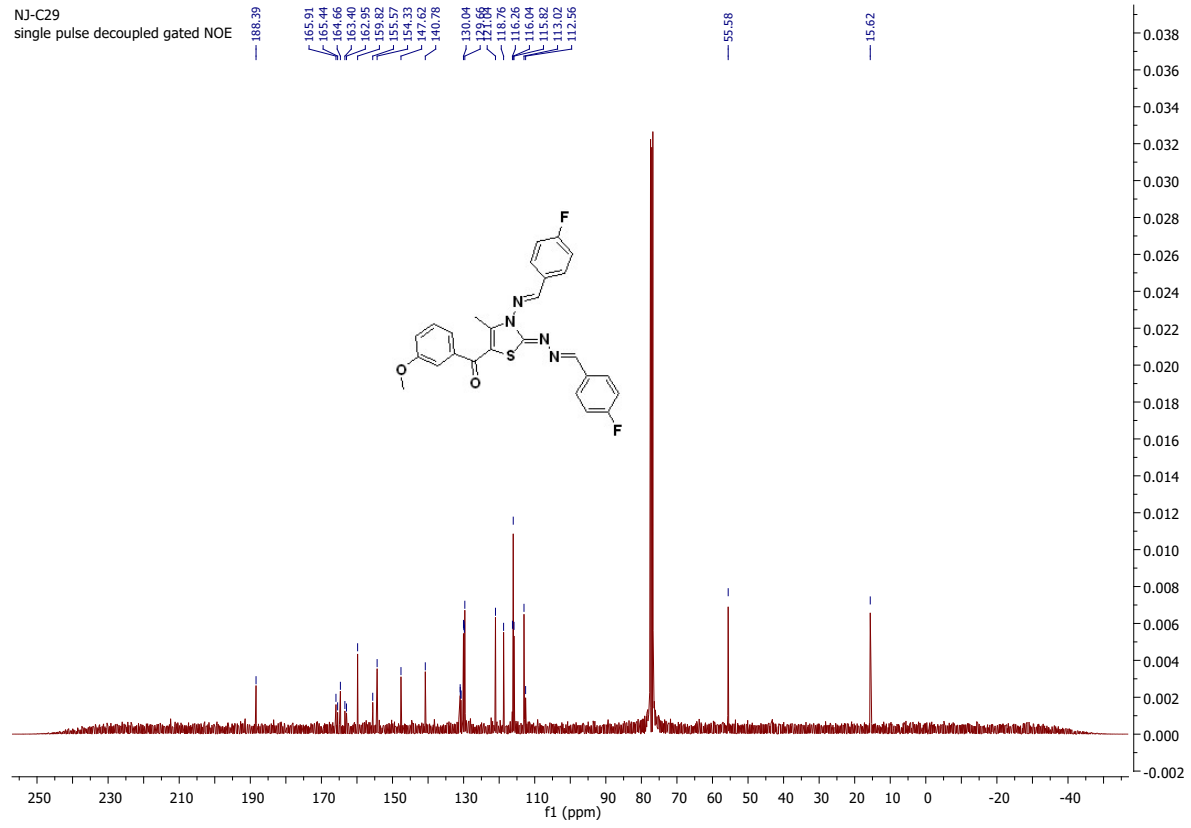

Figure S39. ^{13}C NMR spectrum of 6m

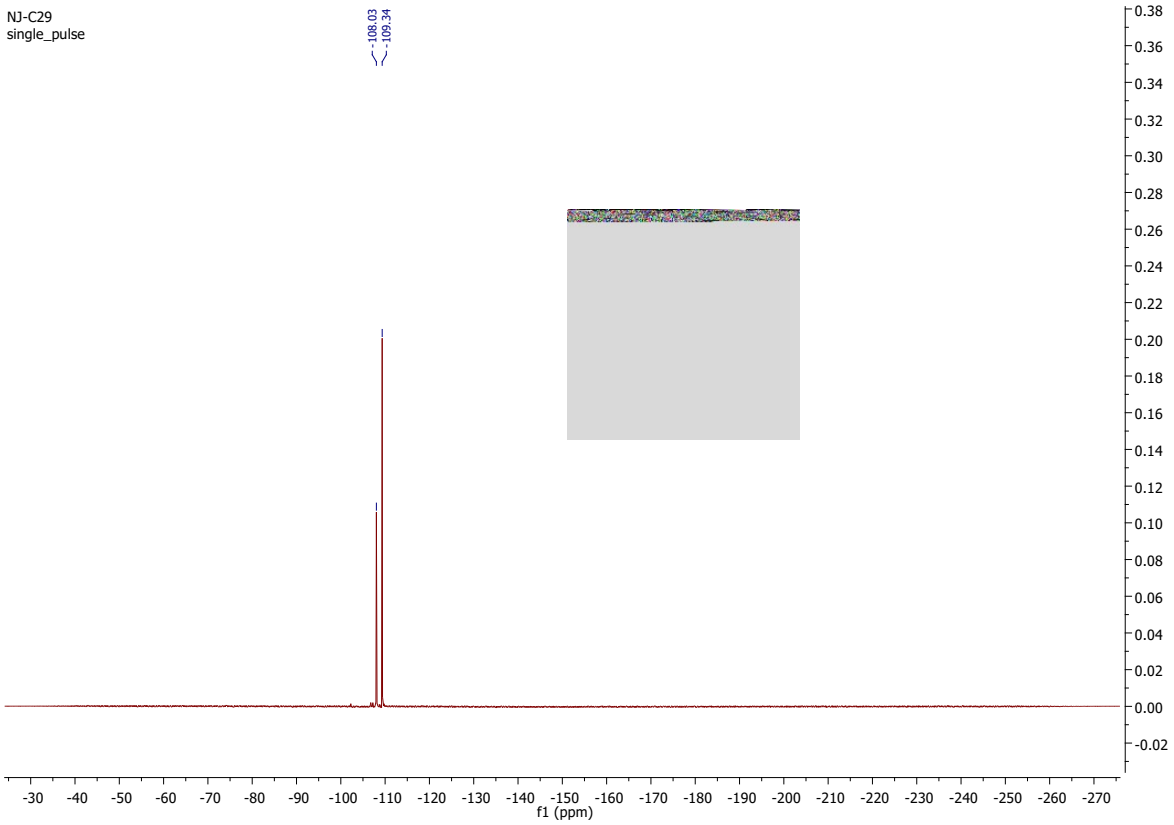

Figure S40. ^{19}F NMR spectrum of 6m

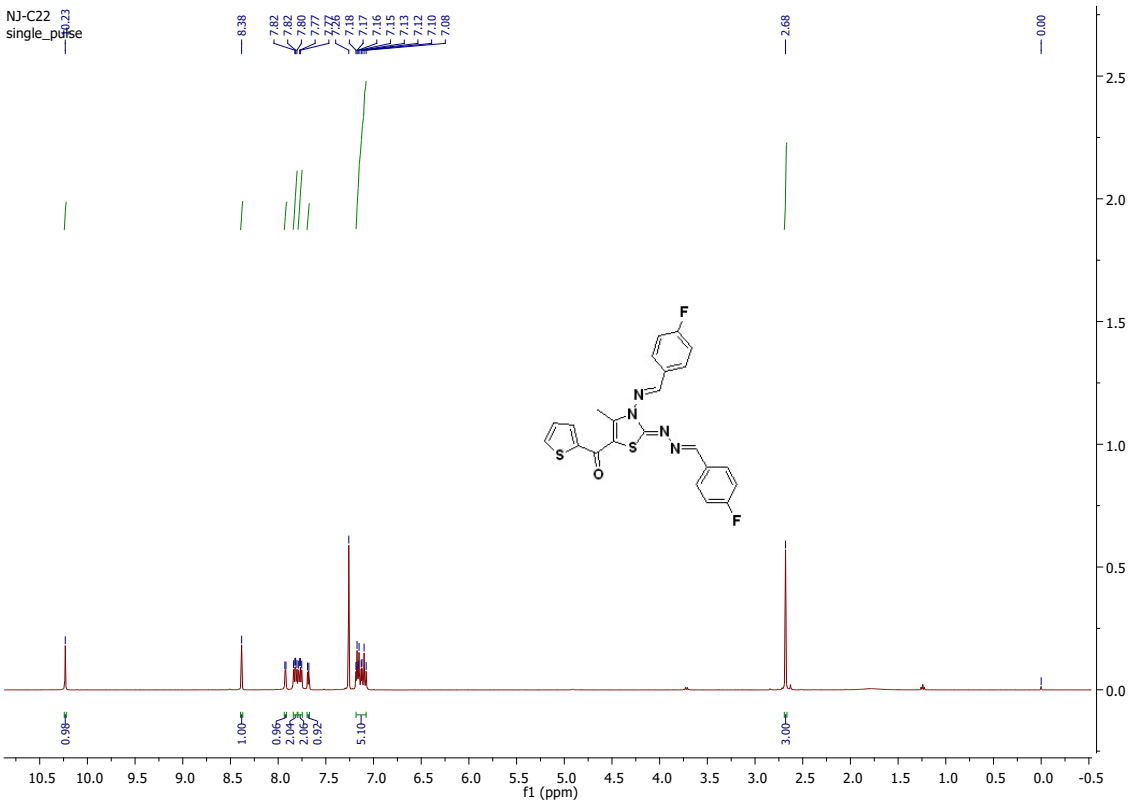

Figure S41. ^{1}H NMR spectrum of 6n

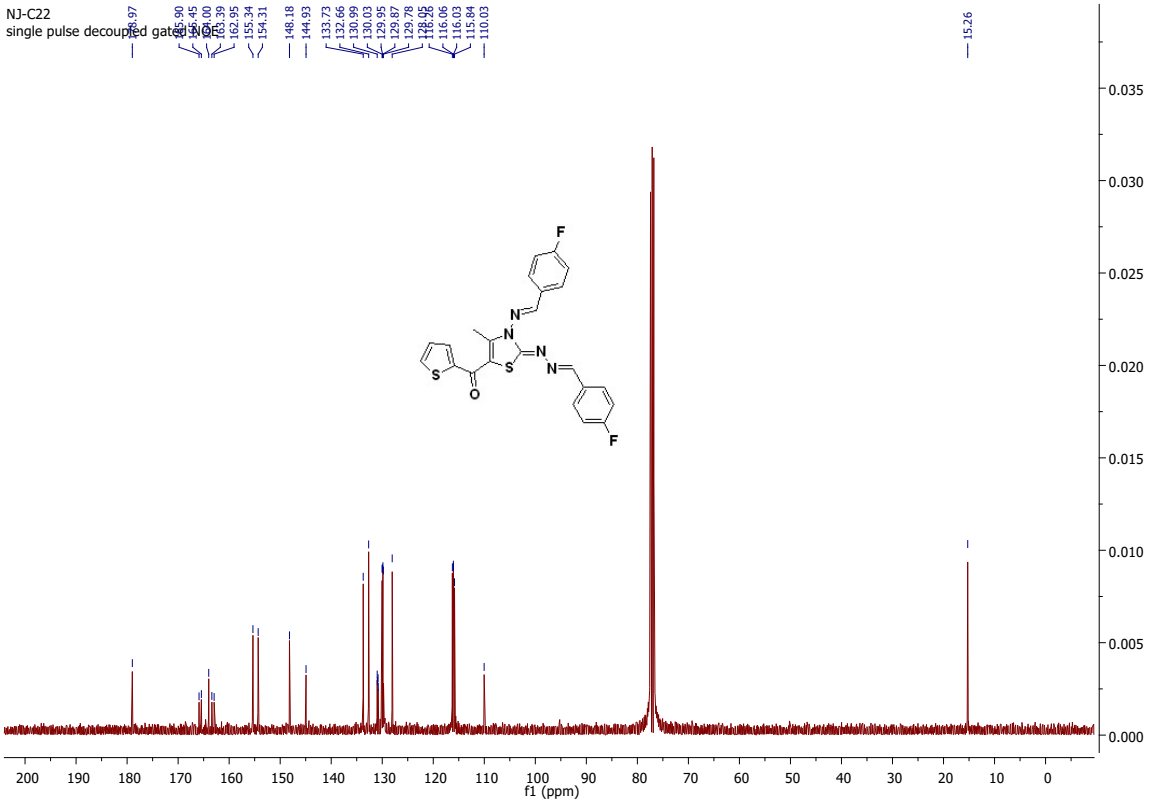

Figure S42. ^{13}C NMR spectrum of 6n

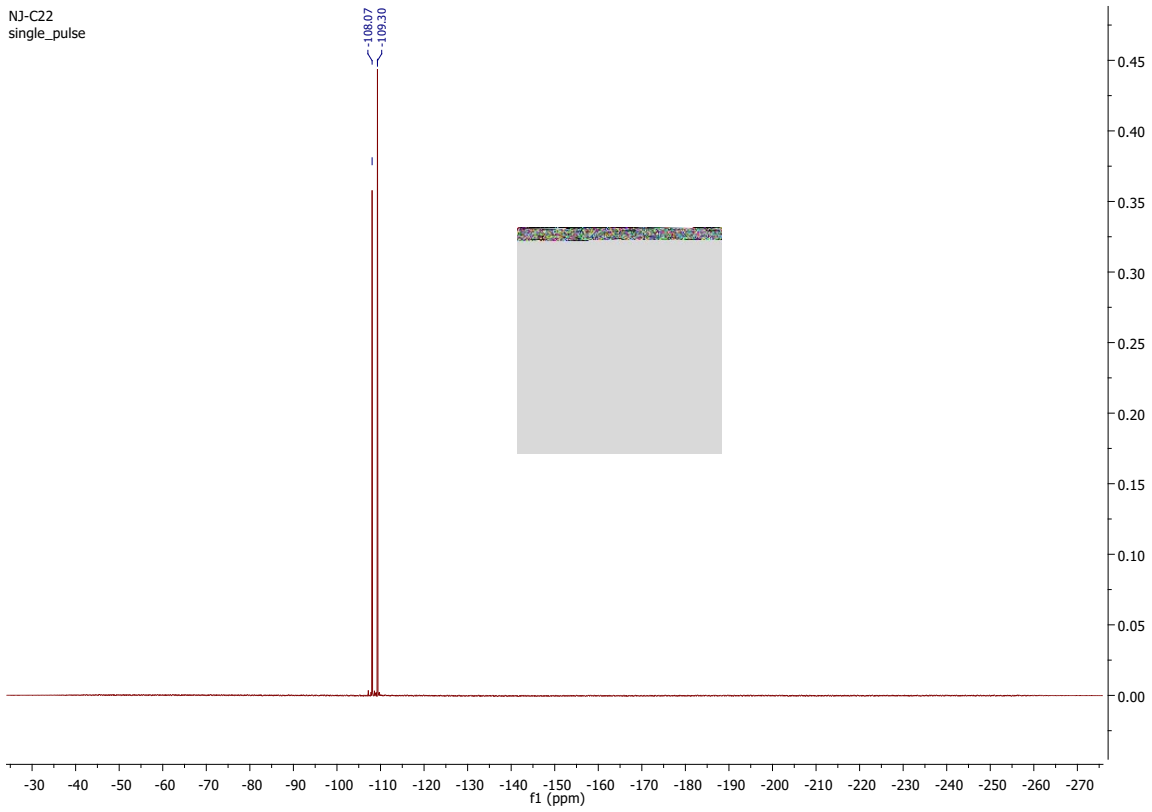

Figure S43. ^{19}F NMR spectrum of 6n